THE MOTION OF MARS' POLE. II. THE EFFECT OF AN ELASTIC MANTLE AND A LIQUID CORE

James L. Hilton

U.S. Naval Observatory, 34th St. and Massachusetts Ave. NW, Washington, DC 20392

ABSTRACT

A first-order approximation of the effects of an elastic mantle and liquid core on the motion of Mars' pole are explored. The effect on Mars' Chandler wobble (Eulerian free nutation) is much less dependent on Mars' structure than the Earth's Chandler wobble depends on the Earth's structure. The period of the liquid core free-core nutation (FCN), however, is found to be very sensitive to the mean core radius; if the FCN period is known with an uncertainty of 2 days, then the mean core radius can be inferred with an uncertainty of only 6 km. The amplitude of the forced nutation in the liquid core models is also sensitive to the mean core radius. The sensitivity is high enough that measuring of the amplitudes of the three largest nutation components with an accuracy of a milliarcsecond will produce measures of the mean core radius with uncertainties of 32, 38, and 67 km, respectively. Elastic mantle, solid core models, however, are found to produce no significant difference in the motion of the pole compared to the rigid solid core model. Evidence for some sort of nonrigid polar motion is shown to exist from the Viking lander radar ranges of Mars. Methods of obtaining higher quality observations of Mars' orientation in space, and the applicability of the methods derived for Mars to other planets in the solar system are discussed.

1. INTRODUCTION

The rigid body precession and nutation of Mars' pole has been discussed in several places such as Struve (1898), de Vaucouleurs (1964), Reasenberg & King (1979), and most recently Hilton (1991). All of these studies are based on a rigid body model for Mars. However, Mars, like the Earth, is not a rigid body, but consists of an elastic mantle and, possibly, a liquid core. The structure of the planet affects its response to both force-free motion such as the Chandler wobble and forced motion such as nutation. The aim of this paper is to explore the effect that an elastic mantle with either a liquid or solid core has on the motion of Mars' pole and how that knowledge can be put to use in gaining a greater understanding of Mars' structure.

For the Earth, the difference between the theoretical rigid structure and the actual elastic Earth with a liquid core causes differences between the observed and predicted amplitude of the Earth's forced nutation components. The physical process of how a liquid in a container affects the motion of the container-liquid system was first constructed by Poinsot (1854). In this case, the liquid is the Earth's outer core and the container is the mantle. However, except in the period of the Chandler wobble, the observations of the motion of the Earth's pole were not accurate enough to show the effects of the elastic, liquid core Earth until the last thirty years. The more recent works, such as those by Wahr (1981a,b, 1982), show that the amplitudes of the forced nutation components resulting from an elastic, liquid core Earth can be modeled as a perturbation to the rigid Earth model theories. This is the approach adopted in the 1980 IAU Theory of Nutation to determine the amplitude of the various nutational elements (Seidelmann *et al.* 1981). These perturbations result in modifications to the nutation of the Earth from about 1% to 0.01% of the theoretical rigid nutation component amplitudes. The largest change in amplitude is about 0″019 for the semiannual nutation term in longitude. Since the 1950's the improvement in the

measurement of the motion of the Earth's pole have made its study a powerful probe of the structure of the Earth (e.g., Kinoshita & Souchay 1990; Zhu *et al.* 1990; Melchior 1986).

The information on the interior of Mars is very sketchy. The only structural information that is certain is (1) Mars' overall physical shape, (2) its mean density, and (3) the structure of the surface gravity field to twelfth degree and order (Christensen & Balmino 1979). Mars' inertia ratio is definitely greater than that of the Earth, but its exact value is subject to debate. Current values range from 0.365 (Reasenberg 1977) to 0.345 (Bills 1989). The seismic experiments that were included in the Viking probes were designed only as a preliminary survey to determine what instruments would be necessary on future missions to Mars. Also, the seismic package functioned properly on only one of the two landers (Anderson *et al.* 1977).

The less extreme central condensation (greater inertia ratio) and small magnetic field are the reasons that some of the existing Mars' models picture a planet with a solid core (Binder & Davis 1973) rather than a liquid core as the Earth has. Most models, however, do use liquid cores, but the composition and mean radius of the core are unknown. Johnston & Toksoz (1977) and Okal & Anderson (1978) discuss the merits of the various possible core configurations. The key to determining the core's composition is determining its mean radius, which will give its mean density based on the planet's inertia ratio.

By using the Earth as an example for how the motion of the pole is affected by a planet's structure and keeping in mind the known and possible differences between Mars and the Earth, it is possible to use the motion of Mars' pole as a probe of its interior structure. The information needed to discriminate between the various models of the Martian interior can be obtained from a few, highly accurate planetary orientation sensors, as opposed to a large net of seismometers needed for a classic determination of the planetary interior structure.

1. REPORT DATE **FEB 1992**	2. REPORT TYPE **N/A**	3. DATES COVERED **-**	
4. TITLE AND SUBTITLE **The Motion of Mars' Pole II. The Effct of An Elastic Mantle and A Liquid Core**		5a. CONTRACT NUMBER	
		5b. GRANT NUMBER	
		5c. PROGRAM ELEMENT NUMBER	
6. AUTHOR(S)		5d. PROJECT NUMBER	
		5e. TASK NUMBER	
		5f. WORK UNIT NUMBER	
7. PERFORMING ORGANIZATION NAME(S) AND ADDRESS(ES) **U.S. Naval Observatory 3450 Massachusetts Avenue, NW Washington, DC 20392**		8. PERFORMING ORGANIZATION REPORT NUMBER	
9. SPONSORING/MONITORING AGENCY NAME(S) AND ADDRESS(ES)		10. SPONSOR/MONITOR'S ACRONYM(S)	
		11. SPONSOR/MONITOR'S REPORT NUMBER(S)	
12. DISTRIBUTION/AVAILABILITY STATEMENT **Approved for public release, distribution unlimited**			
13. SUPPLEMENTARY NOTES			
14. ABSTRACT			
15. SUBJECT TERMS			

16. SECURITY CLASSIFICATION OF:			17. LIMITATION OF ABSTRACT **UU**	18. NUMBER OF PAGES **19**	19a. NAME OF RESPONSIBLE PERSON
a. REPORT **unclassified**	b. ABSTRACT **unclassified**	c. THIS PAGE **unclassified**			

2. THE EFFECTS OF PLANETARY STRUCTURE
ON THE MOTION OF A PLANET

Aside from the Tharsis uplift, Mars has a much simpler surface structure than the Earth. Mars lacks many of the attributes that perturb the Earth's observed polar motion, such as plate tectonics, spin-wobble coupling by surface oceans, and an atmosphere massive enough to contain a significant portion of the planet's angular momentum. These problems have been addressed for the structure of the Earth in numerous papers, such as Dahlen (1976), Wahr (1982), and Wahr & de Vries (1989). The same tools used to handle the more complicated and much better known structure of the Earth can be applied to Mars as a probe of its structure.

The only possibly significant structural complication not accounted for in the above papers is the Tharsis uplift area. Reasenberg (1977) shows that the amount of volcanic activity over this area of Mars' surface may have been great enough that the volcanic shield added to the surface may have shifted Mars' entire center of mass by 800 m with respect to the center of mass of Mars' core.

Normal mode expansion theory (e.g., Smith 1974) shows that a hydrostatic, unstressed, elastic, rotating planet with a solid mantle and a liquid core is subject to three secular and an infinite number of oscillatory modes. The three secular modes compose the linear motion of the planet in space. Of the oscillatory modes, all but three are restricted to the liquid core of the planet. In addition to the normal modes, the Earth also has an annual wobble unconnected with normal mode theory. Hence, except for these four oscillatory modes, the oscillatory modes are unobservable and problematic. The three observable oscillating normal modes are commonly referred to as the tilt over mode, the Chandler wobble, and the free-core nutation. The Chandler wobble, the free-core nutation, and the annual wobble are the three main polar motion components for the Earth. All four modes of these are important enough to discuss in detail.

2.1 The Annual Wobble

The Earth's annual wobble, unlike the other three modes, is not an eigenstate of the motion of the Earth. The annual wobble is a result of the seasonal changes in the surface load resulting from the seasonal shift in the distribution of water over the surface of the Earth from things such as seasonal rains, river runoff, and ice-cap formation. The closest Martian equivalent to the sources of the Earth's annual wobble are the growth and shrinkage of Mars' polar ice caps. However, the ratio of the mass of these ice caps to the mass of the planet is several orders of magnitude smaller than the ratio of the surface water mass with respect to the mass of the Earth, so a martian "annual" term will be insignificant.

2.2 The Tilt Over Mode or TOM

The tilt over mode is the motion of the axis of the rotating coordinate system (mean axis of rotation) about the true axis of rotation. Since this motion is that of a point on the surface of the planet about its rotation axis, this mode has a period identical to the rotation period of the planet. The TOM, by definition, is a retrograde rotation, and is independent of the structure of the planet.
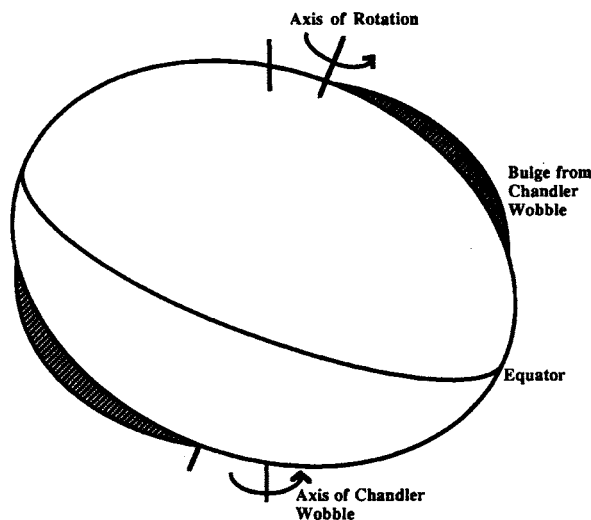
2.3 The Chandler Wobble

The Chandler wobble is the Eulerian free nutation of the planet. It is the physical response to the angular separation between the angular momentum and the angular velocity vectors. The Earth's wobble was first observed by Chandler (1891), but was not recognized as the Eulerian free nutation because the observed period of the motion, 436.0 days (Ooe 1978), is much longer than the predicted rigid Earth period of 304.4 days (Smith & Dahlen 1981). The sources of the large discrepancy between the theoretical, rigid body and measured periods are (1) the elasticity of the Earth's mantle, (2) the size and shape of the core, (3) the tidal motion of the oceans, and (4) inelastic dispersion within the mantle.

First, elasticity results in a considerable lengthening of the rigid body period. The elasticity of the Earth allows the Eulerian nutation to produce a bulge at the equator of rotation of the Chandler wobble (Fig. 1). This secondary bulge, which is the equivalent of a tidal bulge, reduces the effective difference between the principal moments of inertia that are the source of the Eulerian nutation. Although the change in the difference is extremely small, about 0.10% for the Earth, it causes a large increase in the period of the Chandler wobble, 46.98% or 143.0 days (Smith & Dahlen 1981).

Second, the liquid core of a planet causes a decrease in the period of the Chandler wobble. For a long period ($\geqslant$ 1 day), the motions of the core and mantle are weakly coupled because the time for the liquid core to deform itself is short compared to the period of the Chandler wobble (Rochester 1970). Hence, the observed Chandler wobble period is close to the period of a mantle only Chandler wobble. This change causes a decrease of 50.5 days or 16.6% of the rigid solid body Chandler wobble period (Smith & Dahlen 1981).

Third, the Earth's oceans cause an increase of 29.8 days in

Axis of Rotation

Bulge from Chandler Wobble

Equator

Axis of Chandler Wobble

The Effect of Elasticity on the Chandler Wobble

FIG. 1. The Chandler wobble for an elastic planet. For an elastic planet the rotation of the planet about the axis of the Chandler wobble raises a bulge about the equator of the Chandler wobble axis. This bulge reduces the effective difference between the polar and equatorial principal moments of inertia for the planet and increases the period of the Chandler wobble.

the Chandler wobble by reducing the effective difference between the principal moments of inertia of the Earth in the same manner as the elastic mantle. Fortunately, Mars has no oceans, so this effect is ignored.

Fourth, there is the loss of energy through inelastic dispersion in the mantle, that is, the change in the quality factor, Q, with mantle radius (Smith & Dahlen 1981). This contributes a lengthening of the Earth's Chandler wobble of 8.5 days. For Mars the effect of dispersion will be much smaller than it is for the Earth. In the Earth the quality factor ranges from about 350 ± 100 in the lower mantle to about 111 ± 50 in the upper mantle (Smith & Dahlen 1981), so there is as large of a dispersion in Q. However, the overall Q for the Earth is dominated by the lower mantle. In Mars, the overall Q is of the same order as that of the Earth's upper mantle, $50 < Q_{Mars} < 150$ (Smith & Born 1976). The similarity between the Mars' overall Q and the Earth's upper mantle Q suggests that the change in the quality factor with depth for Mars is not as great as it is for the Earth. Thus the dispersion in Mars' mantle will be smaller than it is for the Earth, so the dispersion has a smaller effect on Mars' Chandler wobble.
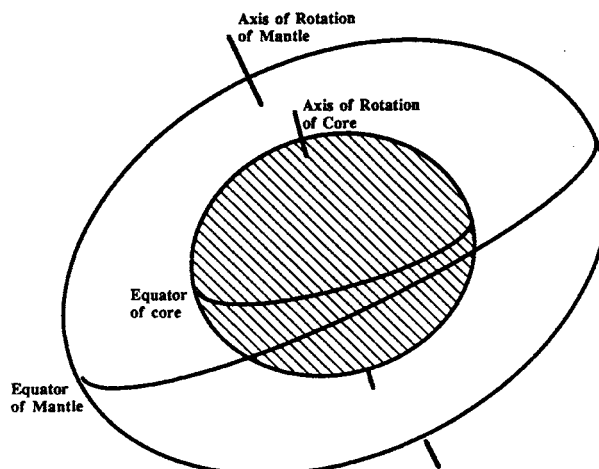
2.4 The Free-Core Nutation or FCN

The nearly diurnal free wobble was first derived by Hough (1895). It is the result of the spheroidal liquid core having a greater mean density than the solid mantle. For a planet near hydrostatic equilibrium, the core's greater density means it has a smaller ellipticity than the mantle. Since the ellipticity of the core is smaller than the mantle, the rate of the Eulerian nutation of the core is slower than the rate of the mantle. However, the difference in the dynamical oblatenesses of the core and the mantle is small, so the difference between their Eulerian nutation rates is also small. Therefore, the alignment between the core and the core cavity is maximized at nearly daily intervals, so the wobble has a nearly diurnal period. Unlike the Chandler wobble, the core does not have sufficient time to deform as the two spheroids (the core and the core cavity in the mantle) nutate. Thus, the pressure at the interface between the core and the mantle changes as the two spheroids move farther from and closer to alignment (Rochester 1970). The change in the pressure over the core-mantle interface creates a wobble in the mantle of the planet (Fig. 2). This is the only significant coupling between the core and the mantle. Associated with this wobble is a much larger nutation with a period of 1/(1—period of wobble) (Rochester et al. 1974). This nutation is the free-core nutation (FCN). Because the associated nutation is much larger than the nearly diurnal free wobble, the FCN is the quantity measured; although the physics is more readily seen in the nearly diurnal free wobble.

For the Earth the period of the FCN should be 461 sidereal days (Wahr 1981b). However, the FCN has never been directly measured. VLBI techniques set an upper limit on the FCN amplitude of $0\overset{''}{.}0033$ (Herring et al. 1988). Although Herring et al. did not directly observe the FCN, its influence on nutation is seen (Zhu et al. 1990).

2.5 The Observable Quantities and Model Parameters

The Chandler wobble, the TOM, and the FCN are the three natural modes of oscillation of a rotating planet with a liquid core and an elastic, solid mantle. The forced nutation components of the planet are driven oscillations of the planetary motion, and the precession is a driven secular motion

Source of the Free Core Nutation

FIG. 2. The source of the free-core nutation. The free-core nutation is a result of the different mean densities of the core and the mantle. Because the core has a greater density than the mantle, rotation of the planet produces a smaller dynamic oblateness for the core than it does for the mantle. The smaller dynamic oblateness results in a slower Eulerian nutation rate for the core than for the mantle. However, since the core is restricted to the cavity inside the mantle, there is a pressure coupling between the core and the mantle that has a nearly diurnal frequency.

about the small circle that is the locus of points for the inclination of the rotation axis of the planet to the orbit of the perturbing body. The ratio between the expected rigid body amplitudes for the nutation and the observed amplitudes are a result of the resonance between the driven oscillations and the natural modes of oscillation of the planet. Since the frequencies of the natural modes of the planet depend on the planetary structure, the amplitude of the nutation will also depend on the structure. Precession, however, is unaffected by the planetary structure, since it is a secular motion of the pole about a small circle on the sky rather than an oscillatory motion.

From the description of the oscillatory modes above and the rigid body nutation developed in Hilton (1991), the fundamental quantities which affect the natural oscillation periods for an oceanless elastic spheroidal planet are (1) the rotation rate of the planet, (2) the polar principal moment of inertia of the mantle, (3) the polar principal moment of inertia of the core, (4) the equatorial principal moment of inertia of the mantle, (5) the equatorial principal moment of inertia of the core, and (6) the elasticity of the mantle. The observable quantities are (1) the rotation rate of the planet, (2) the polar principal moment of inertia of the planet, and (3) the equatorial principal moment of inertia of the planet. The moment of inertia for even a uniform body depends on both the density of the body and its shape, so the known information leaves three unknowns. (1) The ratio of the polar moments of inertia of the mantle and the core, (2) the ratio of the equatorial moments inertia of the mantle and the core, and (3) the elasticity of the mantle. Although there are three oscillatory modes for Mars and three unknowns, the prob-

lem is underdetermined because the TOM adds no useful information. Therefore, it is assumed that the planet is in hydrostatic equilibrium. This assumption is fairly accurate since even small planets such as the Earth are within 1% of overall hydrostatic equilibrium (Smith & Dahlen 1981). Hydrostatic equilibrium allows the ratios of the polar and equatorial principal moments of inertia to be determined once a mean core radius is supplied. Finally, the elasticity of Mars is computed based on the assumption that the mantle of Mars is composed of materials similar enough to the Earth's mantle to provide the same material rigidity. This leaves the mean core radius as the only free variable in the determination of the structure of Mars. Measurements of the Chandler wobble and FCN periods and the amplitudes of the forced nutation terms will each give separate estimates of the mean core radius.

3. THE EFFECT OF MARS' STRUCTURE ON THE MOTION OF ITS POLE

3.1 The Planetary Models

The effect of Mars' structure on its motion is studied using two types of Mars models.

The first model type is based on the models of Okal & Anderson (1978). In these models, Mars is assumed to consist of an elastic mantle with a zero-pressure mean density of about 3–4 gm/cm^3 and a liquid core with a zero-pressure density ranging from 6 to 22 gm/cm^3. The exact core and mantle densities in the models are functions of the mean core radius and the inertia ratio.

These models assume that both the core and the mantle are in hydrostatic equilibrium. Evidence exists, however, that the mantle is about 7% out of hydrostatic equilibrium and the center of mass of the core is offset from the center of mass of the planet by 800 m (Reasenberg 1977). Although this variance from hydrostatic equilibrium is a factor of 4 larger than the same variance for the Earth, it does not cause a significant change in the motion of the pole. The effect of the nonhydrostatic component on the forced nutation of the Earth is only about 1 part in 10^4 (Wahr & de Vries 1989). For Mars, the smallest principal moment of inertia for the core for any of the hydrostatic models is

$$I_C = (1.46 \pm 0.04) \times 10^{34} \text{ kg m}^2,$$

for a core with a mean radius of 800 km, which contains 5.87×10^{22} kg or 0.0915 of the Mars' total mass. The source of the uncertainty in the core moment of inertia for a given mean core radius is the uncertainty in the inertia ratio of Mars. From the parallel axis theorem, the change in the principal moment of inertia caused by the core being moved off center is

$$\Delta I = \mathcal{M}_C d^2, \tag{1}$$

where d is the distance between the center of mass and the rotation axis, and $\mathcal{M}_C$ is the mass of the core (Hestenes 1986). If the axis of rotation of the core is 800 m away from the center of mass, the change in the moment of inertia is

$$\Delta I = (5.87 \times 10^{22} \text{ kg})(800 \text{ m})^2 = 3.76 \times 10^{28} \text{ kg m}^2.$$

The change in the moment of inertia is more than four orders of magnitude smaller than the uncertainty in the moment of inertia. Therefore, until the inertia ratio of Mars is much better known, the effect of the departure from hydrostatic equilibrium is not calculable. The effect of the general departure of the planet from hydrostatic equilibrium on the oscil-

lating normal modes of Mars' core is also smaller than the uncertainty caused by the same variance for the models for the Earth because of Mars' greater dynamic oblateness. The difference between the theoretical and observed Chandler wobble period for the Earth as a result of its departure from hydrostatic equilibrium is 0.5 day (Smith & Dahlen 1981) or 0.25% the uncertainty in the period. Hence, the nonhydrostatic component of Mars is assumed to be insignificant with respect to the motion of Mars' pole.

The second model type is based on the models of Binder & Davis (1973). In these models, both the mantle and the core are solid and elastic. In these models, it is assumed that because of Mars' smaller size, it has cooled enough for the core to solidify. The immediate consequences of the solid core models are (1) the free-core nutation mode disappears and (2) the period of the Chandler wobble increases because both the core and the mantle participate in the wobble, unlike in the liquid core models.

All the models start with a spherical planet with a radius equal to the mean radius of Mars. The input parameters for the models are the mean radius of the core and the percentage of the mass found in the core. The percentage of mass in the core is adjusted, in most models, until the final inertia ratio for the Mars model is 0.3654. The core and mantle densities are computed and used to produce initial profiles for the gravitational potential and the pressure as a function of radius.

The incompressibility of Mars, K, is computed based on the assumption that the material that makes up Mars' mantle, like the Earth's mantle, consists mainly of silicates, so the same empirical equation used to describe the incompressibility of the Earth can be used for Mars. For the mantle and the core, in the solid core models, the incompressibility is given by

$$K = 2.25 \times 10^{11} \text{ Pa} + 3.35p \tag{2}$$

(Stacey 1977) where p is the pressure in Pascals. This function for K represents the Earth's incompressibility to an uncertainty of 2%. For the solid core models, Eq. (2) is used to describe the incompressibility in the core as well as the mantle.

For the liquid core models, the determination for the value K in the core is more difficult. For these models, the value of K is determined from the value of the square of the Brunt–Väisälä frequency,

$$N^2(r) = -g\left(\frac{\rho g}{K} + \rho^{-1}\frac{\partial \rho}{\partial r}\right). \tag{3}$$

Equation (3) describes the motion of a piece of the core material if it is displaced from its equilibrium position. If $N^2(r) > 0$ the displaced portion will oscillate about its equilibrium position, i.e., the core is stably stratified. If $N^2(r) < 0$, then the displaced particle will move away from its equilibrium position (unstable stratification). And if $N^2(r) = 0$, the displaced particle will remain at its displaced position (neutral stratification). The exact state of stratification for the Earth has not been determined (Smith 1977), but neutral stratification, or nearly neutral stratification, is a strong likelihood. Again, appealing to the basic similarity between Mars and the Earth and having no source of information to the contrary, the condition of neutral stratification is applied to the core of Mars.

Incompressibility is defined as the change in density of material with pressure, that is,

$$K = \rho(dp/d\rho). \qquad (4)$$

Since the density of a material is a function of pressure, the density profile needs to be recomputed using the new pressure profile. The rest of the parameters for spherical planet model are then recomputed based on the new density profile. The model is then iterated until it converges. All of the models required, at most, three iterations.

Once the density, gravitational potential, and incompressibility profiles have been determined, the next step is to determine the rigidity and Lamé parameter profiles. The rigidity is also based on the assumption that Mars' mantle and the core, for the solid core models, are composed of materials similar to the Earth. This allows the same empirical relation for the material rigidity of the Earth to be used for Mars (Stacey 1977),

$$\mu = 1.3 \times 10^{11} \text{ Pa} + 1.4p. \qquad (5)$$

For the Earth this approximation has an accuracy of 5%. The Lamé parameter is determined from the incompressibility and the rigidity.

$$1 = K - \tfrac{2}{3}\mu. \qquad (6)$$

The oblateness of a rotating, hydrostatic planet as a function of radius is calculated based on Bullard's (1948) iterative solution of Clairaut's (1743) equation. Clairaut's equation assumes that the planet in question is in hydrostatic equilibrium, which Mars is not. However, the solution to the primordial Mars models of Reasenberg (1977) is extremely close and the difference between the theoretical hydrostatic solution and the measured surface ellipticity of Mars produce errors of less than 0.02%. The main caveat of this extremely good agreement between Reasenberg's primordial Mars model and the hydrostatic equilibrium model is that the amplitudes of the nutation and the precession of the planet depends on the difference between the equatorial and polar moments of inertia, which are very similar; therefore, although the error in the geometric oblateness is extremely small, the error in the dynamical oblateness may be closer to about 8%.

3.2 The Periods of the FCN and Chandler Wobble

From the pressure coupling at the core-mantle interface the angular velocity of the nearly diurnal free wobble (NDFW) is (Rochester *et al.* 1974),

$$\Omega_{\text{NDFW}} = -\Omega A \epsilon_{\text{CM}} / A_{\text{M}} \qquad (7)$$

where ϵ_{CM} is the ellipticity of the core-mantle interface, A is the equatorial moment of inertia for the entire planet, Ω is the angular velocity of the planet, and A_{M} is the equatorial moment of inertia for the mantle alone. The angular velocity of the FCN is computed using period of FCN = 1/(1—period of NDFW) (Rochester *et al.* 1974).

It is much more difficult to calculate the period of the Chandler wobble, however, since its value depends on the determination of the effective dynamical oblateness of the planet. The value of the effective dynamical oblateness is affected by both the planet's elasticity and the coupling between the liquid core and the solid mantle. The effect of the existence of a liquid core upon the Chandler wobble was first quantitatively determined by Hough (1895). Hough (1896) also first solved for the effect of an elastic mantle on the Chandler wobble. The expression of the effects of elasticity on the physical structure of the Earth were later consolidated by Love (1909) and Larmor (1909) into the Love numbers, h and k.

The angular velocity of the Chandler wobble, like the angular velocity of the FCN, is an eigenstate of the normal mode theory, and hence they are both derivable from the theory. However, the FCN period can also be determined using the Hough–Love–Larmor (HLL) theory developed by Smith & Dahlen (1981). This theory is used because it does not require the assumption of hydrostatic equilibrium that normal mode theory requires. Thus, the HLL theory gives an estimate of how much that assumption of hydrostatic equilibrium affects the angular velocity derived. The HLL theory also addresses the motion more directly and gives a better physical feel for what is occurring. The main drawback of the HLL theory is that it is difficult to extend and does not show the connection between the three mantle eigenstates and the higher order core oscillations found in normal mode theory.

In the HLL theory, the angular velocity vector is broken into mean and time varying parts,

$$\boldsymbol{\Omega} = \Omega_1 \hat{\mathbf{e}}_3 + \Omega_1 \mathbf{m}, \qquad (8)$$

where $|\mathbf{m}|$ is small compared to unity and Ω_1 is the mean angular speed. The total angular momentum in inertial space is

$$\mathbf{l}(t) = I(t)\boldsymbol{\Omega}(t) + \mathbf{h}(t) \qquad (9)$$

where the value of $\mathbf{l}(t)$ is independent of the coordinate frame chosen, but the values of I, Ω, and $\mathbf{h}$ are not.

Similarly, the moment of inertia is decomposed into a mean part and a time-varying part,

$$I(t) = I_{\text{r}} + \mathscr{I}(t) \qquad (10)$$

where I_{r} is the rigid body inertia tensor and $\mathscr{I}(t)$ is the time-varying component.

There are now two unknown vectors, $\mathbf{m}$ and $\mathbf{h}$, and an unknown second degree tensor, $\mathscr{I}$, to be solved for. The planet is assumed to be an axisymmetric spheroid. The derivatives of $\mathbf{h}$, $\mathbf{m}$ and $\mathscr{I}$ are of the form $\partial \mathbf{F}/\partial t = i\Omega_{\text{CW}}\mathbf{F}$, and all nonlinear terms in $\mathbf{h}$, $\mathbf{m}$, and ℓ are insignificant. For any motion small enough that the planet's response, $\mathbf{s}$, is linear, the change in rotation, $\mathbf{m}$ is also linear. Hence, since both $\mathscr{I}$ and $\mathbf{h}$ are linear in $\mathbf{s}$, there must be a set of linear relations between $\mathscr{I}$, $\mathbf{h}$, and $\mathbf{m}$, and the solution of the Louiville equation requires knowledge of only $\mathscr{I} \cdot \mathbf{e}_3$

$$\mathscr{I}_{i3} = D_{ij}m_j,$$
$$h_i = \Omega_{\text{CW}}E_{ij}m_j, \qquad (11)$$

where D and E are the linear relations connecting $\mathscr{I}$ and $\mathbf{h}$, respectively, to $\mathbf{m}$.

The axisymmetry of the planet puts restrictions on the degrees of freedom of the coefficients (Dahlen 1976) for the linear relations in Eqs. (11). These restrictions are

$$D_{ij} = D(\delta_{i1}\delta_{j1} + \delta_{i2}\delta_{j2}) + D'\delta_{i3}\delta_{j3} \qquad (12)$$

and

$$E_{ij} = E(\delta_{i1}\delta_{j1} + \delta_{i2}\delta_{j2}) + iE'\epsilon_{ij3} + E''\delta_{i3}\delta_{j3}, \qquad (13)$$

where δ_{ij} is the Kronecker delta, ϵ_{ijk} is the Levi–Civita density tensor, and D, D', E, E', and E'' are all real scalars.

The parameters $m_j \ll 1$, so m_3, which only appears for rotations about the mean axis of rotation is insignificant in comparison to Ω and, hence, it can be set to zero. The linear portion of the solution is then

$$\Omega_{\rm CW} \approx \frac{C - A - D}{A + D + E + E'} \Omega. \tag{14}$$

The determination of the angular speed and period of the Chandler wobble has been reduced to determining the values of the three parameters, D, E, and E'. D is the only parameter connected to the change in the inertia tensor, so it alone determines the effect of the elasticity of the planet on the Chandler wobble. The parameters E and E' are connected with the change in the angular momentum of the observed mantle; that is, their values are determined by the effect of the core-mantle coupling on the Chandler wobble.

The deformation response of a planet to a wrench, that is a combined force and torque, depends on the material response to the wrench. Dahlen (1976) shows that to first order the equation for the parameter D is

$$D = \frac{k_2 \Omega^2 a^5}{3G}. \tag{15}$$

The value of k_2 is determined either from direct measurements of the planet tide or can be calculated from the normal mode solution for the planet model. For the Mars' models the value of k_2 was calculated using the method developed by Longman (1962, 1963).

The zeroth order effect of the fluid core, represented by E and E', on the Chandler wobble is immediately seen by making the assumptions that the core is spherical and that the core-mantle interface is frictionless. In this case, the Chandler wobble observed for a rigid mantle will be that for the mantle alone. That is,

$$\Omega_{\rm CW} = \frac{A_{\rm M} - C_{\rm M}}{A_{\rm M}} \Omega \tag{16}$$

where $C_{\rm M}$ and $A_{\rm M}$ are the polar and equatorial moments of inertia of the mantle alone. However, since the core is spherical, the moments of inertia of the core are equal, $A_{\rm C} = C_{\rm C}$, so the angular velocity of the Chandler wobble is given by

$$\Omega_{\rm CW} = \frac{A - C}{A_{\rm M}} \Omega. \tag{17}$$

The parameter E' in Eq. (14) for the case of a spherical, frictionless fluid core is then

$$E' = -A_{\rm C}. \tag{18}$$

Rochester (1970) shows that the assumption of a frictionless core-mantle interface is a good assumption. However, the assumption of a spherical core-mantle interface is not a good approximation. When the core is assumed to be oblate, the mechanism of pressure coupling is added. This coupling is the result of a normal force between the core and the mantle. The normal force results from the change in orientation of the mantle relative to the core. Hough (1895) and Smith & Dahlen (1981) show that the effect of pressure coupling at the elliptical core mantle interface is given to first order by

$$E' = -(1 - \epsilon_{\rm c})A_{\rm C}, \tag{19}$$

where $\epsilon_{\rm C}$ is the dynamical ellipticity of the core. Using these values for the parameters in Eq. (14) gives the angular velocity of the Chandler wobble as

$$\Omega_{\rm CW} = \frac{C - A - D}{A_{\rm M} + \epsilon_{\rm C} A_{\rm C} + D} \Omega. \tag{20}$$

Although many simplifications have been made in determining the value for $\Omega_{\rm CW}$, comparison of the linear function

in Eq. (20) with more exact iterative solutions for the Chandler wobble using normal mode theory show differences of only 0.06%, which is much smaller than the uncertainties of the parameters used in the solution.

Smith & Dahlen (1981) show that the Chandler wobble for the Earth determined using the above solution gives a period that is comparable to the measured value of the Chandler wobble period to within about half a day. The changes caused by elasticity and a liquid core on Mars' Chandler wobble are found to be significantly smaller than those for the Earth for two reasons. First, because of Mars' smaller size the planet is more rigid than the Earth, hence the value of k_2 is smaller. This means the tidal bulge raised on Mars is proportionately smaller than it is for the Earth, so the proportionate sizes of the products of inertia for Mars are smaller. Second, Mars has a greater inherent dynamical ellipticity than the Earth. Therefore, since the period of the Chandler wobble depends on the effective dynamical ellipticity, a given absolute change in the dynamical ellipticity of Mars has a smaller effect on the Chandler wobble than the same change on the Earth does.

3.3 Results for Liquid Core Mars Models

Liquid core planetary models were produced with mean core radii at intervals of 100 km from 800 to 2000 km. The ratio of core to mantle mass for most of the models was varied until the value of the inertia ratio was 0.3654 (Reasenberg 1977). Four mean core radii were chosen for more intensive study. Those mean core radii were 800, 1500, 1700, and 2000 km. The criteria used to determine which mean radii would be studied in detail are (1) the zero pressure density for the core of the 800 km model is 22.418 g/cm^3. This density is much greater than the zero pressure density of either nickel (8.90 g/cm^3) or iron (7.86 g/cm^3), the most likely dense components to be found in the core, and only slightly less than that of osmium (22.48 g/cm^3), the densest known naturally occurring substance. Therefore, the core density at a mean core radius of 800 km is an absolute lower bound for the mean core radius. (2) At a mean radius of 2000 km, the zero pressure density of the core has decreased to only 5.334 g/cm^3, significantly less than that of the expected core constituents. In addition, the core now has a radius that is 60% that of the entire planet, so the 2000 km core radius model represents a reasonable upper bound to the size of the core. The mean core radius of 1500 km was chosen to give a model with a mean core radius that is halfway in between the radii of the two extreme cases. The core with the mean radius of 1700 km was chosen so that the models developed here could be directly comparable with the main Mars model of Okal & Anderson (1978).

The 1700 km mean core radius Mars model is shown in Table 1. In this table columns 1 and 7 give the identification number of each of the tabulated radii in the model; column 2, the mean radius; column 3, the geometric flattening; column 4, the density at the tabulated radius; column 5, the total mass enclosed by the radius; column 6, the gravitational acceleration at the radius; column 8, the pressure at the radius; column 9, the equatorial radius; column 10, the incompressibility at the tabulated radius; column 11, the Lamé parameter at the model tabulated radius; and column 12, the $k_2 + 1$ Love number.

Table 2 shows the change in model results as various parameters are adjusted. In the second section, where the inertia ratio is varied, the equatorial radius changes from 3392.8

TABLE 1. Fluid core Mars model with a mean core radius of 1700 km.

No.	Mean Radius (km)	Flattening	Density (kg/m^3)	Total Mass (kg)	Grav. Acell. (m/s^2)
0	0.0	0.000000	7086.8	0.000E+00	0.0000
1	100.0	0.003882	7085.5	2.968E+19	0.1980
2	200.0	0.003883	7081.6	2.373E+20	0.3959
3	300.0	0.003884	7075.1	8.004E+20	0.5934
4	400.0	0.003886	7065.9	1.896E+21	0.7904
5	500.0	0.003887	7054.0	3.698E+21	0.9869
6	600.0	0.003889	7039.5	6.381E+21	1.1827
7	700.0	0.003898	7022.2	1.012E+22	1.3775
8	800.0	0.003914	7002.1	1.507E+22	1.5714
9	900.0	0.003930	6979.2	2.142E+22	1.7642
10	1000.0	0.003944	6953.4	2.931E+22	1.9556
11	1100.0	0.003957	6924.6	3.891E+22	2.1456
12	1200.0	0.003967	6892.7	5.037E+22	2.3340
13	1300.0	0.003977	6857.7	6.385E+22	2.5206
14	1400.0	0.003986	6819.3	7.947E+22	2.7053
15	1500.0	0.003994	6777.6	9.738E+22	2.8878
16	1600.0	0.004002	6732.3	1.177E+23	3.0680
17	1700.0	0.004010	6683.3	1.406E+23	3.2457
18	1800.0	0.004032	3664.2	1.547E+23	3.1856
19	1900.0	0.004080	3649.9	1.704E+23	3.1493
20	2000.0	0.004144	3635.7	1.878E+23	3.1320
21	2100.0	0.004216	3621.4	2.069E+23	3.1303
22	2200.0	0.004292	3606.9	2.279E+23	3.1410
23	2300.0	0.004370	3592.3	2.507E+23	3.1621
24	2400.0	0.004447	3577.4	2.755E+23	3.1917
25	2500.0	0.004521	3562.2	3.024E+23	3.2284
26	2600.0	0.004592	3546.7	3.314E+23	3.2709
27	2700.0	0.004659	3530.8	3.626E+23	3.3183
28	2800.0	0.004722	3514.4	3.960E+23	3.3697
29	2900.0	0.004781	3497.6	4.317E+23	3.4246
30	3000.0	0.004837	3480.3	4.697E+23	3.4823
31	3100.0	0.004889	3462.4	5.102E+23	3.5423
32	3200.0	0.004937	3444.0	5.532E+23	3.6042
33	3300.0	0.004982	3425.0	5.986E+23	3.6676
34	3387.2	0.005019	3407.9	6.404E+23	3.7240

No.	Pressure (Pa)	Equatorial Radius (km)	μ (Pa)	Lambda (Pa)	k + 1
0	3.972E+10	0.0	0.0	3.559E+11	
1	3.965E+10	100.1	0.0	3.557E+11	0.0011
2	3.943E+10	200.3	0.0	3.551E+11	0.0044
3	3.908E+10	300.4	0.0	3.540E+11	0.0098
4	3.860E+10	400.5	0.0	3.524E+11	0.0175
5	3.797E+10	500.6	0.0	3.505E+11	0.0273
6	3.720E+10	600.8	0.0	3.480E+11	0.0392
7	3.630E+10	700.9	0.0	3.452E+11	0.0533
8	3.527E+10	801.0	0.0	3.419E+11	0.0695
9	3.410E+10	901.2	0.0	3.382E+11	0.0879
10	3.281E+10	1001.3	0.0	3.340E+11	0.1083
11	3.139E+10	1101.5	0.0	3.294E+11	0.1307
12	2.984E+10	1201.6	0.0	3.243E+11	0.1552
13	2.817E+10	1301.7	0.0	3.188E+11	0.1817
14	2.638E+10	1401.8	0.0	3.129E+11	0.2101
15	2.448E+10	1502.0	0.0	3.065E+11	0.2405
16	2.247E+10	1602.1	0.0	2.997E+11	0.2727
17	2.035E+10	1702.3	0.0	2.925E+11	0.3068
18	1.869E+10	1802.4	1.562E+11	1.828E+11	0.3416
19	1.753E+10	1902.6	1.545E+11	1.801E+11	0.3792
20	1.639E+10	2002.8	1.529E+11	1.775E+11	0.4185
21	1.525E+10	2103.0	1.513E+11	1.749E+11	0.4597
22	1.412E+10	2203.2	1.498E+11	1.723E+11	0.5028
23	1.298E+10	2303.4	1.482E+11	1.697E+11	0.5479
24	1.184E+10	2403.6	1.466E+11	1.670E+11	0.5951
25	1.070E+10	2503.8	1.450E+11	1.643E+11	0.6445
26	9.542E+09	2604.0	1.434E+11	1.616E+11	0.6960
27	8.376E+09	2704.2	1.417E+11	1.589E+11	0.7497
28	7.198E+09	2804.4	1.401E+11	1.561E+11	0.8056
29	6.007E+09	2904.6	1.384E+11	1.532E+11	0.8638
30	4.802E+09	3004.8	1.367E+11	1.503E+11	0.9242
31	3.583E+09	3105.1	1.350E+11	1.473E+11	0.9869
32	2.349E+09	3205.3	1.333E+11	1.442E+11	1.0520
33	1.100E+09	3305.5	1.315E+11	1.411E+11	1.1193
34	0.000E+00	3392.8	1.300E+11	1.383E+11	1.1800

TABLE 2. Significant properties of liquid core models for Mars.

		(Change in Core Size)				
Mean Core Radius (km)	Equatorial Radius (km)	Zero Pressure Core (kg/m^3)	Density Mantle (kg/m^3)	k	Free Core Nutation (day^{-1})	Chandler Wobble (day^{-1})
800.0	3392.9	22418.5	3487.1	0.1695	-0.0016253	0.0062530
1500.0	3392.8	7149.6	3434.3	0.1589	-0.0039235	0.0061637
1700.0	3392.8	6180.0	3407.9	0.1800	-0.0043778	0.0060624
2000.0	3392.8	5333.9	3351.3	0.2271	-0.0050508	0.0059476

All models were calculated with a value for q (the polar inertia divided by the mass times the radius squared) of 0.3654.

		(Change in Core Density)				
q (km)	Equatorial Radius (km)	Zero Pressure Core (kg/m^3)	Density Mantle (kg/m^3)	k	Free Core Nutation (day^{-1})	Chandler Wobble (day^{-1})
0.3452	3392.4	7693.9	3157.1	0.1691	-0.0037205	0.0064053
0.3644	3392.8	6256.9	3395.4	0.1794	-0.0043405	0.0060834
0.3654	3392.8	6180.0	3407.9	0.1800	-0.0043778	0.0060624
0.3664	3392.8	6108.3	3419.5	0.1805	-0.0044129	0.0060424

All models were calculated with a mean core radius of 1700 km.

		(Change in Rigidity, μ, and/or Bulk Modulus, K, as a function of pressure)				
parameter (km)	Equatorial Radius (km)	Zero Pressure Core (kg/m^3)	Density Mantle (kg/m^3)	k	Free Core Nutation (day^{-1})	Chandler Wobble (day^{-1})
standard	3392.8	6180.0	3407.9	0.1800	-0.0043778	0.0060624
Δμ (5%)	3392.8	6180.0	3407.9	0.1788	-0.0043778	0.0060676
ΔK (2%)	3392.8	6182.1	3408.0	0.1811	-0.0043776	0.0060572
Δμ , ΔK	3392.8	6182.1	3408.4	0.1799	-0.0043776	0.0060625

All models were calculated with a mean core radius of 1700 km and a q of 0.3654.

km for the Reasenberg (1977) value for the inertia ratio, 0.3654, to 3392.4 km for the Bills (1989) inertia ratio of 0.3452. The measured equatorial diameter for Mars is 3393.4 km (Davies *et al.* 1985), so the Reasenberg value for the inertia ratio does not require as large a nonhydrostatic component for Mars' structure as the Bills value for the iner-

tia ratio. This indicates a preference for the Reasenberg value of the inertia ratio.

3.3.1 The Chandler wobble

The period of the Chandler wobble for a rigid Mars with a solid center is simply

$$T_{CW} = \frac{2\pi}{\hat{e} \cdot \Omega} \frac{A}{A - C}. \tag{21}$$

Using the values of e, Ω, A, and C for Mars in Hilton (1990, 1991), the rigid body Chandler wobble period is

$$T_{CW} = 154.6 \text{ days},$$

corresponding to a frequency of

$$f_{CW} = 0.006468 \text{ day}^{-1}.$$

This period is about half of the Earth's theoretical rigid Chandler wobble period of 303.4 days (Smith & Dahlen 1981).

The effect of the various modifications going from a rigid body Chandler wobble to the Chandler wobble for an elastic mantle, liquid core Mars model are made using a mean core radius of 1700 km or 1/2 of the mean radius of Mars. This model is compared with the Smith & Dahlen (1981) Earth model. Introducing the liquid core in the Earth model reduces the period of the Chandler wobble to 253.9 days, a reduction of 50.5 days from the rigid Earth model. For Mars, however, a liquid core 1700 km in mean diameter reduces the period of the Chandler wobble to 145.2 days, a reduction of only 9.4 days, even though the ratio of the core and mantle radii is comparable to the same ratio for the Earth. Changing the character of the mantle from rigid to elastic in the model increases the period of the Martian Chandler wobble by only 19.5 days, to a period of 164.7 days. This is much smaller than the 143.0 day increase that an elastic mantle adds to the period of the Earth's Chandler wobble. The reason for the

much smaller effect of planetary elasticity on the Chandler wobble. The reason for the much smaller effect of planetary elasticity on the Chandler wobble period is Mars' higher rigidity.

The third source of change in the Chandler wobble period for Mars is dispersion within the mantle. This modification causes only a small change in the period because the change in the quality factor with radius for Mars is much smaller than the uncertainty in the quality factor (Smith & Born 1976). The small change in the quality factor means that the dispersion effect on the Chandler wobble period is unknown, but it is probably insignificant. The effect of the quality factor on the motion of Mars' pole will be discussed in more detail in Sec. *3.3.3*.

The change in the frequency of the Chandler wobble as a function of the various model parameters is given in Tables 2 and 3. The latter table shows the Chandler wobble frequency as a function of mean core radius tabulated at 100 km intervals from a core radius of 800–2000 km. The additional model values for the Chandler wobble period are shown, since it is obvious from the four standard models that the frequency is nonlinear (Fig. 3). The frequency of the wobble is sensitive to the change in the core radius (5.13% change over the range of core size) and change in the inertia ratio of Mars (6.01% change in q). However, the range for q includes the rather large central condensation determined by Bills (1989), which is not likely, given the arguments by Kaula *et al.* (1989). Limiting the uncertainty in q to that of Reasenberg (1977), the range for the frequency of the Chandler wobble due to uncertainty in q is only 0.68%. Over the entire range of core models, the frequency of the Chandler wobble is determined empirically to within 2% of its actual value by

$$f_{CW} = 0.004523 + 1.141 \times 10^{-6}r - 2.978 \times 10^{-9}r^2$$
$$+ 6.320 \times 10^{-13} \ r^3, \tag{22}$$

where r is the radius of the core in kilometers. For core radii of 1100–2000 km the relation between the frequency of the
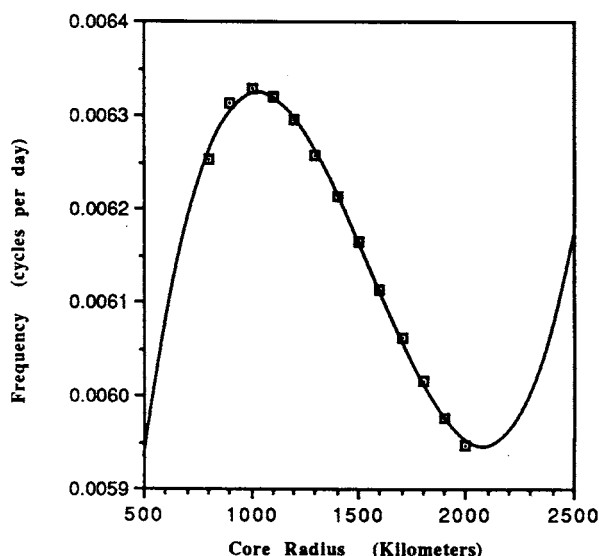

Chandler Wobble Frequency

FIG. 3. The liquid core Chandler wobble frequency as a function of mean core radius. The frequency of the Chandler wobble for a liquid core, elastic Mars' models is computed with mean core radii from 800 to 2000 km in radius (squares). The change in frequency with radius is nonlinear, but it is well fitted by a cubic polynomial (line). If the uncertainty in the period is 2 days and the frequency is less than 0.00625 day^{-1}, the radius of the core can be determined to an accuracy of 180 km. The frequency does not correspond to a unique radius at frequencies greater than 0.00625 day^{-1}.

Chandler wobble and the radius of the core is nearly linear and approximated by

$$f_{CW} = 0.006812 - 4.322 \times 10^{-6}r. \tag{23}$$

However, a given frequency for the Chandler wobble does not correspond to a single core radius for frequencies greater than about 0.00625 day^{-1}.

The best determination of the Chandler wobble period for the Earth (Smith & Dahlen 1981) has an uncertainty of 2.0 days. Assuming that the Chandler wobble period of Mars can be determined with the same uncertainty, the radius of the core can be determined from the Chandler wobble only with an uncertainty of 180 km if the mean core radius is greater than 1300 km.

There are three reasons why the Chandler wobble of Mars is less sensitive to the planet's structure than the Earth's Chandler wobble is to the Earth's structure.

First, the inherent dynamical oblateness of Mars is a factor of 1.814 greater than that of the Earth. The larger dynamical oblateness is evident in Mars' higher rigid body Chandler wobble frequency. Therefore, to have the equivalent effect on Mars, a modification to the basic Chandler wobble must be nearly a factor of two larger than the equivalent modification to the Chandler wobble theory for the Earth.

Second, the ratio of the moment of inertia of the core to the moment of inertia of the entire planet for all of the models are either smaller than, or approximately equal to, the same ratio for the Earth. Thus, the effect of the abstinence of the core from the Chandler wobble for Mars will be smaller than the similar effect is for the Earth.

TABLE 3. Frequency of the Chandler wobble of Mars as a function of the core radius (liquid core).

Core Radius (km)	Chandler Wobble (day^{-1})
800	0.0062530
900	0.0063126
1000	0.0063291
1100	0.0063209
1200	0.0062953
1300	0.0062584
1400	0.0062138
1500	0.0061637
1600	0.0061126
1700	0.0060624
1800	0.0060161
1900	0.0059766
2000	0.0059476

Third, the value for the Love number, k_2, for Mars is only 0.18 in comparison to the Earth's k_2 of 0.35. This smaller value of k_2 is expected from the Love (1909) approximation for k_2,

$$k_2 = \frac{3}{2}\left(1 + \frac{19\mu}{2g\rho R}\right)^{-1},$$

$$\approx \frac{3g\rho R}{19\mu}; \quad \frac{19\mu}{2g\rho R} \gg 1, \tag{24}$$

where μ is the rigidity of the material of which the planet is composed, g is the gravitational acceleration at the surface, ρ is the mean density of the planet, and R is the mean radius. The gravitational acceleration, mean density, and mean radius of Mars are all smaller than the same quantities for the Earth. The assumption that both the Earth and Mars are composed of similar materials means that the material rigidity of the two planets will be the same. Therefore, the right-hand side of Eq. (24) and the value of k_2 is smaller for Mars than it is for the Earth. The smaller value for k_2 means that, for a comparable amount of exterior force, the ratio of deformation of Mars from the force with the deformation resulting from Mars' rotation is significantly smaller for Mars than it is for the Earth. Thus, the ratio of the change in the difference between the polar and equatorial moments of inertia resulting from an exterior force with respect to the hydrostatic difference is smaller for Mars than for the Earth, and the effect of elasticity is smaller for Mars than for the Earth.

3.3.2 The free-core nutation

In the Earth, the free-core nutation itself appears to be unexcited. Again assuming that Mars is similar to the Earth, it is not likely that the FCN can be directly detected for Mars either. If, on the other hand, the lack of a detectable FCN is a peculiarity of the Earth alone, then the FCN frequency for Mars would be extremely useful in determining the size of Mars' core. First, the sensitivity of the FCN to changes in the inertia ratio of the planet is much smaller than the sensitivity of Mars' Chandler wobble (Table 2). The change in the Chandler wobble frequency from one extreme to the other of the value for inertia ratio is 119% of the change in the frequency over the extremes in the core size of the model. However, the change in the frequency of the FCN over the extremes in inertia ratio is only 20% of the change of frequency over the extremes in the core size. The FCN is also less sensitive to uncertainties in the elasticity of the planet, so the FCN is less affected by the two greatest sources of uncertainty in the Mars models. Second, the FCN period, unlike the Chandler wobble, is a nearly linear function of the mean core radius and is single valued over the range in model core sizes (Fig. 4 and Table 2). The negative sign preceding the frequencies in the table denotes that the free-core nutation is a retrograde (clockwise) motion of the pole. Finally, the slope of the mean core radius–frequency relation is steep enough to allow the radius of the core to be determined to an uncertainty of only 6 km if the uncertainty in the FCN period is 2 days.

3.3.3 Nutation

The smaller k_2 Love number reduces the effect of elasticity on the Chandler wobble. But the smaller k_2 also means Mars' normal mode oscillations have a greater effect on the
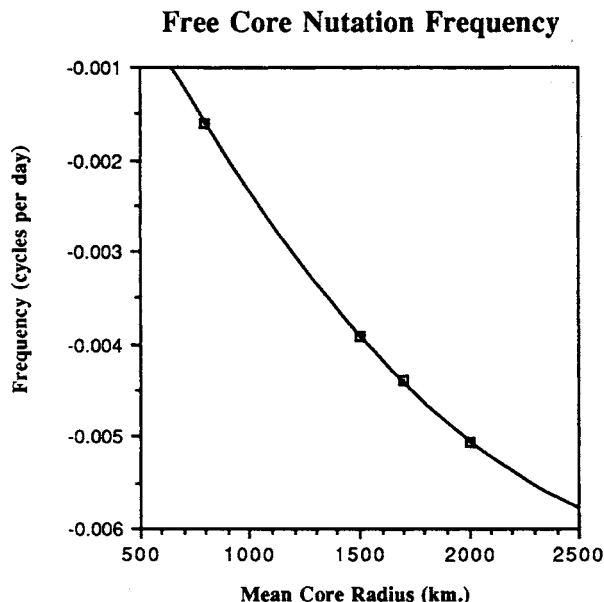

FIG. 4. The frequency of the free-core nutation (FCN) as a function of mean core radius. The FCN period as a function of the mean core radii between 800 and 2000 km. Only the four closely studied models are shown. Unlike the Chandler wobble the FCN is nearly linear (the line fit to the data shown is quadratic) with core radius. The change in frequency with core radius is quite steep. If the period of the FCN is known with an accuracy of 2 days, the mean core radius can be determined to an uncertainty of only 6 km.

amplitude of the nutation of Mars than the Earth's normal mode oscillations have on the Earth. This is seen clearly in Table 4, which shows the amplitude of the nutation components as a function of the change in the mean radius of the core. This phenomenon can be understood in terms of the quality factor, Q. The quality factor is defined as

$$Q \equiv 2\pi \frac{\text{Total Energy}}{\text{Energy Dissipated per Cycle}}. \tag{25}$$

For the liquid core Mars models the two sources of dissipation in the Chandler wobble will be core-mantle coupling processes and inelasticity of the mantle of the planet.

The first of these two sources an be immediately ruled out as a source of significant damping. The estimates for the value of Q, based on the largest estimates available for the known core-mantle coupling mechanisms for the Earth, is greater than or equal to 12 000 (Smith & Dahlen 1981). Again, because Mars is similar to the Earth in its structure, the estimate for dissipation between the core and the mantle should hold for Mars. Even if the structural differences between the Earth and Mars are large, the strength of the core-mantle coupling mechanisms for Mars need to be more than an order of magnitude greater than they are in the Earth before they would become a significant source of damping.

Smith & Dahlen (1981) show from the normal mode perturbation theory that the amount of energy in the Chandler wobble lost to friction is related by a complicated function to the rigidity and the Lamé parameter. However, the relationship between Q and the rigidity is also an inverse relationship, as is the relationship between k_2 and rigidity. There-

TABLE 4. Nutation amplitudes for different liquid core models of Mars.

(Different Core Sizes)

Nutation in Obliquity

Period (day)	Rigid	800 km	1500 km	1700 km	2000 km
			Core Size		
686.72	-0.0493	-0.0419	-0.0435	-0.0439	-0.0444
343.41	0.5158	0.4687	0.4793	0.4824	0.4866
228.96	0.1130	0.1074	0.1089	0.1094	0.1100
171.72	0.0193	0.0189	0.0191	0.0191	0.0192
137.38	0.0030	0.0030	0.0030	0.0030	0.0030
686.93	-0.0004	-0.0003	-0.0004	-0.0004	-0.0004
828.5	-0.0040	-0.0034	-0.0035	-0.0035	-0.0036
19850	-0.0028	-0.0022	-0.0023	-0.0023	-0.0024

Nutation in Longitude

Period (day)	Rigid	800 km	1500 km	1700 km	2000 km
			Core Size		
686.72	-0.1407	-0.1197	-0.1240	-0.1252	-0.1268
343.41	1.0962	0.9962	1.0186	1.0251	1.0340
228.96	0.2401	0.2283	0.2315	0.2324	0.2338
171.72	0.0409	0.0402	0.0405	0.0406	0.0408
137.38	0.0634	0.0639	0.0641	0.0642	0.0643
114.48	0.0009	0.0010	0.0010	0.0010	0.0009
686.93	-0.6357	-0.5409	-0.5603	-0.5657	-0.5730
343.46	-0.0445	-0.0404	-0.0414	-0.0416	-0.0420
228.98	-0.0041	-0.0039	-0.0039	-0.0039	-0.0040
828.5	-0.23	-0.19	-0.20	-0.20	-0.21
19850	-0.060	-0.046	-0.049	-0.049	-0.050

All models were calculated with a value for q of 0.3654.

(Change in Core Density)

Nutation in Obliquity

Period (day)	0.3452	0.3644	0.3654	0.3664
		q		
686.72	-0.0433	-0.0439	-0.0439	-0.0439
343.41	0.4840	0.4829	0.4824	0.4818
228.96	0.1110	0.1096	0.1094	0.1092
171.72	0.0195	0.0191	0.0191	0.0191
137.38	0.0031	0.0030	0.0030	0.0030
686.93	-0.0004	-0.0004	-0.0004	-0.0004
828.5	-0.0035	-0.0035	-0.0035	-0.0035
19850	-0.0022	-0.0023	-0.0023	-0.0023

All models were calculated with a core diameter of 1700 km.

(Change in Core Density)

Nutation in Longitude

Period (day)	0.3452	0.3644	0.3654	0.3664
		q		
686.72	-0.1236	-0.1252	-0.1252	-0.1252
343.41	1.0294	1.0264	1.0251	1.0238
228.96	0.2358	0.2329	0.2324	0.2320
171.72	0.0416	0.0407	0.0406	0.0405
137.38	0.0661	0.0644	0.0642	0.0640
114.48	0.0010	0.0010	0.0010	0.0010
686.93	-0.5585	-0.5658	-0.5657	-0.5655
343.46	-0.0418	-0.0417	-0.0416	-0.0416
228.98	-0.0040	-0.0040	-0.0039	-0.0039
828.5	-0.20	-0.20	-0.20	-0.20
19850	-0.047	-0.049	-0.049	-0.049

All models were calculated with a core diameter of 1700 km.

(Change in Rigidity, μ and/or Bulk Modulus, K as a function of Pressure)

Nutation in Obliquity

Period (day)	standard	$\Delta\mu$ (5%)	ΔK (2%)	$\Delta\mu$, ΔK
			parameter	
686.72	-0.0439	-0.0439	-0.0439	-0.0439
343.41	0.4824	0.4824	0.4823	0.4824
228.96	0.1094	0.1094	0.1094	0.1094
171.72	0.0191	0.0191	0.0191	0.0191
137.38	0.0030	0.0030	0.0030	0.0030
686.93	-0.0004	-0.0004	-0.0004	-0.0004
828.5	-0.0035	-0.0035	-0.0035	-0.0035
19850	-0.0023	-0.0023	-0.0023	-0.0023

Nutation in Longitude

Period (day)	standard	$\Delta\mu$(5%)	ΔK (2%)	$\Delta\mu$, ΔK
			parameter	
686.72	-0.1252	-0.1252	-0.1252	-0.1252
343.41	1.0251	1.0252	1.0250	1.0251
228.96	0.2324	0.2324	0.2324	0.2324
171.72	0.0406	0.0406	0.0406	0.0406
137.38	0.0642	0.0642	0.0642	0.0642
114.48	0.0010	0.0010	0.0010	0.0010
686.93	-0.5657	-0.5658	-0.5655	-0.5657
343.46	-0.0416	-0.0416	-0.0416	-0.0416
228.98	-0.0039	-0.0039	-0.0039	-0.0039
828.5	-0.20	-0.20	-0.20	-0.20
19850	-0.049	-0.049	-0.049	-0.0055

All models were calculated with a core diameter of 1700 km.

fore, the relationship between Q and k_2 is a direct relation. Smith & Born (1976) show that, for Mars, this relation is approximately linear. Since Mars' k_2 is smaller than the Earth's, Mars is expected to have a lower quality factor than the Earth. Smith & Born's (1976) determination, based on the change in the orbital motion of Phobos, indicates a Q of

$$50 < Q_{\text{Mars}} < 150,$$

which is much smaller than the Q of the Earth found by Smith & Dahlen (1981) of

$$350 < Q_{\text{Earth}} < 600.$$

For lightly damped systems,

$$Q \approx \Omega_T / \delta\Omega, \tag{26}$$

where Ω_T is the resonance frequency of the system and $\delta\Omega$ is the frequency interval on the resonance curve when the amplitude is $\sqrt{2}/2$ of its maximum. Thus, the range of frequen-

cies over which the amplitudes of the nutation components for Mars will be affected by the resonance with a normal mode oscillation will be 2.3–12 times wider than the range of frequencies in nutation that are affected by a normal mode oscillations of the Earth. The amplitude of the nutation components as a function of the mean core radius are given in Table 4.

The change of the forced nutation amplitudes with the mean radius of the core, like the frequency of the FCN, is nearly linear. In Fig. 5 the change in amplitude with mean core radius is plotted for the three largest nutation components (two in longitude and one in obliquity). Measurements of the amplitudes of these three nutation components to an accuracy of 0".001 produce estimates of the mean core radius with uncertainties of 67, 38, and 32 km. The uncertainty of the core radius found from the mean of all three measurements is 28 km. There are a total of five nutation components that change significantly over the range of the

sin $\mathcal{L}$

(a)

cos 2 Λ sin 2 $\mathcal{L}$

(b)

Nutation in Obliquity
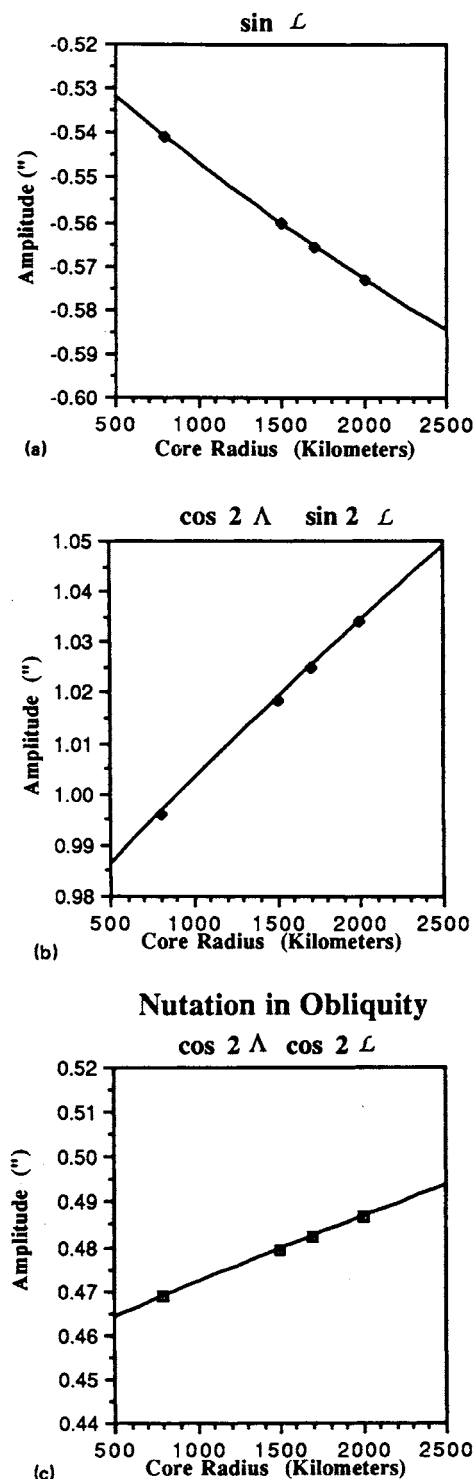### cos 2 Λ cos 2 $\mathcal{L}$

(c)

FIG. 5. (a, b) The amplitudes of the two largest Martian nutation components in longitude as a function of mean core radius. (c) The amplitude of the largest Martian nutation in latitude as a function of the mean core radius. All three of the nutation amplitudes are plotted with mean core radii varying from 800 to 2000 km. All have significant, nearly linear, changes in their amplitudes with core radius. Measuring the amplitudes of these nutation components with an accuracy of 0″001 determines the mean core radius to an accuracy of 67, 32, and 38 km, respectively.

models at the milliarcsecond level, and three of those change at the 10 milliarcsec level. Also, there is little chance of confusing the amplitudes of a fluid core Mars with those of the rigid model for Mars, since the difference between the fluid core, elastic models and the rigid Mars' model can be as large as 0″1 (main 343.5 day component in longitude) and is larger than 0″04 for two nutation components in longitude (main 343.5 day and secondary 687.0 day components) and one nutation in obliquity, 343.5 day component (Table 4)!

The nutation in longitude driven by the motion of Phobos' node (Hilton 1990, 1991) may also be usable as an indicator of the radius of Mars' core, since the amplitude is fairly large and its period is rather short. However, before it can be used as a core radius indicator, the two largest sources of uncertainty in its amplitude (the rate of motion of Phobos' node and Phobos' mass) need to be known with at least an order of magnitude greater precision.

A test for the effect of the uncertainties in the rigidity and the bulk modulus profiles used in the models on the amplitude of the nutation is made by computing three variations of the 1700 km radius core model. The three variations are (1) bulk modulus increased by 2%, (2) rigidity increased by 5%, and (3) both the bulk modulus increased by 2% and the rigidity increased by 5%. The absolute difference between the nutation amplitude in the standard model and the varied models were all less than 0.1 milliarcsec (Table 4).

The change in the Mars' principal moment of inertia has an effect on the amplitude of the nutation only an order of magnitude larger than the uncertainty in the rigidity and compressibility parameters (Tables 2 and 4). Its greatest effect is on the main 343.5 day nutation in longitude with a change of 5.6 milliarcsec from extremum to extremum. Using just the uncertainty in the Reasenberg (1977) value for the inertia ratio, the largest uncertainty for the main 343.5 day nutation in longitude is only ± 1.3 milliarcsec.

Therefore, the liquid core Mars models show it is possible to determine the size of the core to 70 km or less from the amplitudes of several of the nutation components and from the period of the free-core nutation, if it is excited. Neither the nutation components nor the FCN are significantly affected by the uncertainties in the rigidity and compressibility of the planet's materials or the uncertainty in the inertia ratio. The Chandler wobble can determine the core radius with an uncertainty of 180 km for mean core radii greater than 1300 km if the period is known with an uncertainty of 2 days. For mean core radii less than 1300 km, the frequency of the Chandler wobble is not unique.

3.4 Solid Core Mars Models

Like the liquid core models, the primary solid core models are calculated with mean core radii of 800, 1500, 1700, and 2000 km. The ratio of the core to mantle mass is varied until the value for the inertia ratio, q, for the standard models is 0.3654.

The results for the model with a 1700 km mean core radius are given in Table 5. The identical radial profiles for the flattening, density, total mass, gravitational acceleration, pressure, and equatorial radius for both the solid core and the liquid core models is expected since all the models use the assumption that Mars is in hydrostatic equilibrium. The only differences between the basic solid core and liquid core models are (1) the value for the rigidity in the core, μ, is not 0 but continues to increase according to the empirical formula given in Eq. (2), and (2) the value of the Lamé parameter

TABLE 5. Solid core Mars model with a mean core radius of 1700 km.

No.	Mean Radius (km)	Flattening	Density (kg/m^3)	Total Mass (kg)	Grav. Acell. (m/s^2)
0	0.0	0.000000	7086.8	0.000E+00	0.0000
1	100.0	0.003882	7085.5	2.968E+19	0.1980
2	200.0	0.003883	7081.6	2.373E+20	0.3959
3	300.0	0.003884	7075.1	8.004E+20	0.5934
4	400.0	0.003886	7065.9	1.896E+21	0.7904
5	500.0	0.003887	7054.0	3.698E+21	0.9869
6	600.0	0.003889	7039.5	6.381E+21	1.1827
7	700.0	0.003898	7022.2	1.012E+22	1.3775
8	800.0	0.003914	7002.1	1.507E+22	1.5714
9	900.0	0.003930	6979.2	2.142E+22	1.7642
10	1000.0	0.003944	6953.4	2.931E+22	1.9556
11	1100.0	0.003957	6924.6	3.891E+22	2.1456
12	1200.0	0.003967	6892.7	5.037E+22	2.3340
13	1300.0	0.003977	6857.7	6.385E+22	2.5206
14	1400.0	0.003986	6819.3	7.947E+22	2.7053
15	1500.0	0.003994	6777.6	9.738E+22	2.8878
16	1600.0	0.004002	6732.3	1.177E+23	3.0680
17	1700.0	0.004010	6683.3	1.406E+23	3.2457
18	1800.0	0.004032	3664.2	1.547E+23	3.1856
19	1900.0	0.004080	3649.9	1.704E+23	3.1493
20	2000.0	0.004144	3635.7	1.878E+23	3.1320
21	2100.0	0.004216	3621.4	2.069E+23	3.1303
22	2200.0	0.004292	3606.9	2.279E+23	3.1410
23	2300.0	0.004370	3592.3	2.507E+23	3.1621
24	2400.0	0.004447	3577.4	2.755E+23	3.1917
25	2500.0	0.004521	3562.2	3.024E+23	3.2284
26	2600.0	0.004592	3546.7	3.314E+23	3.2709
27	2700.0	0.004659	3530.8	3.626E+23	3.3183
28	2800.0	0.004722	3514.4	3.960E+23	3.3697
29	2900.0	0.004781	3497.6	4.317E+23	3.4246
30	3000.0	0.004837	3480.3	4.697E+23	3.4823
31	3100.0	0.004889	3462.4	5.102E+23	3.5423
32	3200.0	0.004937	3444.0	5.532E+23	3.6042
33	3300.0	0.004982	3425.0	5.986E+23	3.6676
34	3387.2	0.005019	3407.9	6.404E+23	3.7240

No.	Pressure (Pa)	Equatorial Radius (km)	μ (Pa)	Lambda (Pa)	k + 1
0	3.972E+10	0.0	1.856E+11	2.322E+11	
1	3.965E+10	100.1	1.855E+11	2.321E+11	0.0011
2	3.943E+10	200.3	1.852E+11	2.316E+11	0.0043
3	3.908E+10	300.4	1.847E+11	2.308E+11	0.0094
4	3.860E+10	400.5	1.840E+11	2.297E+11	0.0164
5	3.797E+10	500.6	1.832E+11	2.283E+11	0.0254
6	3.720E+10	600.8	1.821E+11	2.266E+11	0.0364
7	3.630E+10	700.9	1.808E+11	2.246E+11	0.0495
8	3.527E+10	801.0	1.794E+11	2.223E+11	0.0645
9	3.410E+10	901.2	1.777E+11	2.197E+11	0.0816
10	3.281E+10	1001.3	1.759E+11	2.167E+11	0.1007
11	3.139E+10	1101.5	1.739E+11	2.134E+11	0.1218
12	2.984E+10	1201.6	1.718E+11	2.098E+11	0.1449
13	2.817E+10	1301.7	1.694E+11	2.059E+11	0.1700
14	2.638E+10	1401.9	1.669E+11	2.016E+11	0.1971
15	2.448E+10	1502.0	1.643E+11	1.970E+11	0.2261
16	2.247E+10	1602.1	1.615E+11	1.921E+11	0.2572
17	2.035E+10	1702.3	1.585E+11	1.868E+11	0.2871
18	1.869E+10	1802.4	1.562E+11	1.828E+11	0.3164
19	1.753E+10	1902.6	1.545E+11	1.801E+11	0.3485
20	1.639E+10	2002.8	1.529E+11	1.775E+11	0.3828
21	1.525E+10	2103.0	1.513E+11	1.749E+11	0.4194
22	1.412E+10	2203.2	1.498E+11	1.723E+11	0.4581
23	1.298E+10	2303.4	1.482E+11	1.697E+11	0.4989
24	1.184E+10	2403.6	1.466E+11	1.670E+11	0.5417
25	1.070E+10	2503.8	1.450E+11	1.643E+11	0.5866
26	9.542E+09	2604.0	1.434E+11	1.616E+11	0.6334
27	8.376E+09	2704.2	1.417E+11	1.589E+11	0.6821
28	7.198E+09	2804.4	1.401E+11	1.561E+11	0.7328
29	6.007E+09	2904.6	1.384E+11	1.532E+11	0.7855
30	4.802E+09	3004.8	1.367E+11	1.503E+11	0.8400
31	3.583E+09	3105.1	1.350E+11	1.473E+11	0.8965
32	2.349E+09	3205.3	1.333E+11	1.442E+11	0.9549
33	1.100E+09	3305.5	1.315E+11	1.411E+11	1.0152
34	0.000E+00	3392.8	1.300E+11	1.383E+11	1.0692

in the core is not based on the assumption that it is neutrally stable, but follows Eq. (3) as it does in the mantle.

Although it has little effect on the immediate shape, pressure, and density of the planet, the assumption of a solid core for Mars has a very profound effect on the elasticity of the

planet, as seen by comparing column 12 of Table 5 with column 12 of Table 1. The Love number k_2 at the surface of Mars is reduced by a factor of about 2 for the solid core model. In short, the overall elasticity of the solid core planet model is about half of that of the liquid core planet model. Therefore, the effect of planetary elasticity on the amplitude of the forced nutation will be much smaller for the solid core case than it was for the liquid core models. Although a lower k_2 is indicative of a lower Q and, hence, a wider range of frequencies over which the amplitudes of forced oscillations are affected, it also means that the magnitude of the resonance effect is reduced (Table 6).

The third immediately obvious difference between the solid core and liquid core models for Mars is the absence of the free-core nutation for the solid core model. The FCN cannot exist in the solid core models since it is the result of the pressure coupling between the core and the mantle caused by the difference in the Eulerian precession rates of the liquid core and the solid mantle.

3.4.1 The Chandler wobble

The effect of the lower planetary elasticity and the solid core participation in the Chandler wobble is very pronounced. The Chandler wobble period for the solid core models are much closer to the rigid Mars Chandler wobble period than to the periods of the liquid core models. For example, the frequency for a core with a mean diameter of 1700 km is

$$f_{\rm CW} = 0.0065624 \text{ day}^{-1}.$$

TABLE 6. Significant properties of solid core models from Mars.

		(Change in Core Size)			
Mean Core Radius (km)	Equatorial Radius (km)	Zero Pressure Density Core (kg/m^3)	Mantle (kg/m^3)	k	Chandler Wobble (day^{-1})
800.0	3392.9	22418.5	3487.1	0.1110	0.0065030
1500.0	3392.8	7149.6	3434.3	0.0714	0.0065496
1700.0	3392.8	6180.0	3407.9	0.0692	0.0065624
2000.0	3392.8	5333.9	3351.3	0.0673	0.0067146

All models were calculated with a value for q (the polar inertia divided by the mass times the radius squared) of 0.3654.

		(Change in Core Density)			
q	Equatorial Radius (km)	Zero Pressure Density Core (kg/m^3)	Mantle (kg/m^3)	k	Chandler Wobble (day^{-1})
0.3452	3392.4	7693.9	3157.1	0.0686	0.0068963
0.3644	3392.8	6256.9	3395.4	0.0692	0.0065837
0.3654	3392.8	6180.0	3407.9	0.0692	0.0065624
0.3664	3392.8	6108.3	3419.5	0.0693	0.0065429

All models were calculated with a mean core radius of 1700 km.

		(Change in Rigidity, μ, and/or Bulk Modulus, K, as a function of pressure)			
parameter (km)	Equatorial Radius (km)	Zero Pressure Density Core (kg/m^3)	Mantle (kg/m^3)	k	Chandler Wobble (day^{-1})
standard	3392.8	6180.0	3407.9	0.0692	0.0065624
$\Delta\mu$ (5%)	3392.8	6180.0	3407.9	0.0678	0.0065690
ΔK (2%)	3392.8	6182.1	3408.0	0.0700	0.0065589
$\Delta\mu$, ΔK	3392.8	6182.1	3408.4	0.0685	0.0065655

All models were calculated with a mean core radius of 1700 km and a q of 0.3654.

This frequency differs from the rigid body frequency by only 9.4×10^{-5} day^{-1}, while the difference between the solid core and the liquid core frequency is 5.00×10^{-4} day^{-1}.

The change of frequency with mean core radius given in Table 7 and Fig. 6 is much smaller than for the liquid core models. Also, like the liquid core models, the relation between the frequency of the Chandler wobble and the core size is definitely nonlinear. Like the liquid core model Chandler wobble, the solid core model Chandler wobble can also be characterized by an empirical cubic function,

$$f_{CW} = \begin{cases} 0.0060766 + 5.33 \times 10^{-7} r; & 800 \text{ km} < r < 900 \text{ km}, \\ 0.0054706 + 6.22 \times 10^{-7} r; & 1800 \text{ km} < r < 2000 \text{ km}. \end{cases} \tag{28}$$

Because the rate of change of the Chandler wobble frequency with mean core radius is much lower for the solid core models than for the liquid core models, a measurement of the period of the Chandler wobble with an uncertainty of 2 days leads to an uncertainty in the mean core radius of 1700 km in the 800 km $< r <$ 900 km range and 1400 km in the 1800 km $< r <$ 2000 km range. Therefore, the frequency of the Chandler wobble is not a usable indicator of the mean core radius for a solid core Mars.

The frequency of the Chandler wobble, shown in Table 6, is rather insensitive to the uncertainties in the rigidity and compressibility of the materials that make up the planet. The frequency changes only 6.6×10^{-6} day^{-1} from one extreme to the other. Also, like the liquid core models, the solid core models of Mars are insensitive to the inertia ratio of the planet. The only significant frequency change is for the extreme inertia ratio of Bills (1989). The change in the frequency with inertia ratio is linear over the entire range of q.

3.4.2 Nutation

Table 8 gives the amplitudes of the nutation components for the solid core, elastic Mars models. The amplitudes are

$$f_{CW} = 0.0049341 + 3.8610 \times 10^{-6} r - 2.968 \times 10^{-9} r^2 + 7.413 \times 10^{-13} r^3, \tag{27}$$

where the mean radius, r, is in kilometers and the frequency is in day^{-1}. The range over which the frequency corresponds to a single value of the mean core radius is small (800 km $< r <$ 900 km and 1800 km $< r <$ 2000 km). Over these two ranges the value of the Chandler wobble as a function of radius can be calculated using

shown, as with the liquid core models, for changes in the size of the core, the rate of change in the incompressibility and rigidity with pressure, and the inertia ratio of the planet. The amplitudes of the nutation components are affected by neither the mean core radius nor the uncertainty in the rigidity and incompressibility. In fact, to the number of significant digits given, there is no difference in nutation amplitude between the solid core, elastic Mars models and the rigid Mars model.

TABLE 7. Frequency of the Chandler wobble of Mars as a function of the mean core radius (solid core).

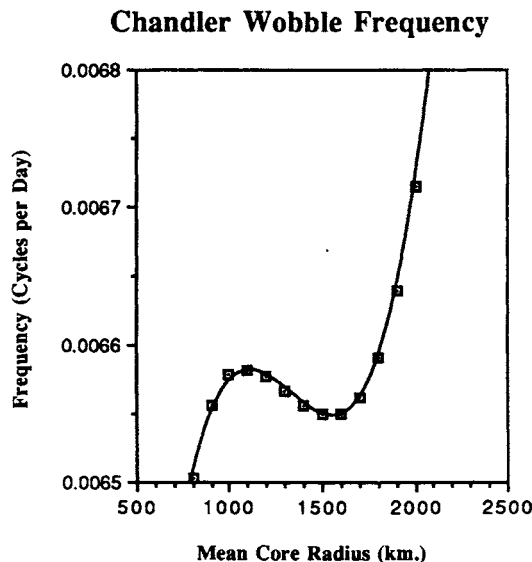| Core Radius (km)	Chandler Wobble (day^{-1})
800	0.0065030
900	0.0065563
1000	0.0065785
1100	0.0065817
1200	0.0065772
1300	0.0065668
1400	0.0065562
1500	0.0065496
1600	0.0065505
1700	0.0065624
1800	0.0065902
1900	0.0066394
2000	0.0067146

Chandler Wobble Frequency

FIG. 6. The solid core Chandler wobble frequency as a function of the mean core radius. The frequency of the Chandler wobble for solid core, elastic Mars models is computed with mean core radii from 800 to 2000 km in radius (squares). The change in frequency with radius is nonlinear, but it is well fitted by a cubic polynomial (line). If the uncertainty in the period is 2 days and the frequency is not between 0.00655 and 0.0066 day^{-1} the radius of the core can be determined to an accuracy of between 1400 and 1700 km. The frequency does not correspond to a unique radius at frequencies between 0.00655 and 0.00660 day^{-1}.

TABLE 8. Nutation amplitudes for different solid core models of Mars.

(Different Core Sizes)

Nutation in Obliquity

Period (day)	Rigid	800 km	1500 km	1700 km	2000 km
			Core Size		
686.72	-0.0493	-0.0493	-0.0493	-0.0493	-0.0493
343.41	0.5158	0.5158	0.5158	0.5158	0.5158
228.96	0.1130	0.1130	0.1130	0.1130	0.1130
171.72	0.0193	0.0193	0.0193	0.0193	0.0193
137.38	0.0030	0.0030	0.0030	0.0030	0.0030
686.93	-0.0004	-0.0004	-0.0004	-0.0004	-0.0004
828.5	-0.0040	-0.0040	-0.0040	-0.0040	-0.0040
19850	-0.0028	-0.0028	-0.0028	-0.0028	-0.0028

Nutation in Longitude

Period (day)	Rigid	800 km	1500 km	1700 km	2000 km
			Core Size		
686.72	-0.1407	-0.1407	-0.1407	-0.1407	-0.1407
343.41	1.0962	1.0962	1.0962	1.0962	1.0962
228.96	0.2401	0.2401	0.2401	0.2401	0.2401
171.72	0.0409	0.0409	0.0409	0.0409	0.0409
137.38	0.0634	0.0634	0.0634	0.0634	0.0634
114.48	0.0009	0.0009	0.0009	0.0009	0.0009
686.93	-0.6357	-0.6357	-0.6357	-0.6357	-0.6357
343.46	-0.0445	-0.0445	-0.0445	-0.0445	-0.0445
228.98	-0.0041	-0.0041	-0.0041	-0.0041	-0.0041
828.5	-0.23	-0.23	-0.23	-0.23	-0.23
19850	-0.060	-0.060	-0.060	-0.060	-0.060

All models were calculated with a value for q of 0.3654.

(Change in Core Density)

Nutation in Obliquity

Period (day)	0.3452	0.3644	0.3654	0.3664
			q	
686.72	-0.0507	-0.0494	-0.0493	-0.0492
343.41	0.5309	0.5170	0.5158	0.5148
228.96	0.1163	0.1133	0.1130	0.1128
171.72	0.0198	0.0193	0.0193	0.0192
137.38	0.0031	0.0030	0.0030	0.0030
686.93	-0.0004	-0.0004	-0.0004	-0.0004
828.5	-0.0041	-0.0040	-0.0040	-0.0040
19850	-0.0029	-0.0028	-0.0028	-0.0028

All models were calculated with a core diameter of 1700 km.

(Change in Core Density)

Nutation in Longitude

Period (day)	0.3452	0.3644	0.3654	0.3664
			q	
686.72	-0.1448	-0.1410	-0.1407	-0.1404
343.41	1.1282	1.0987	1.0962	1.0941
228.98	0.2471	0.2407	0.2401	0.2396
171.72	0.0421	0.0410	0.0409	0.0408
137.38	0.0653	0.0635	0.0634	0.0633
114.48	0.0010	0.0009	0.0009	0.0009
686.93	-0.6543	-0.6371	-0.6357	-0.6344
343.46	-0.0458	-0.0446	-0.0445	-0.0444
228.96	-0.0042	-0.0041	-0.0041	-0.0041
828.5	-0.24	-0.23	-0.23	-0.23
19850	-0.062	-0.060	-0.060	-0.060

All models were calculated with a core diameter of 1700 km.

(Change in Rigidity, mu and/or Bulk Modulus, K as a function of Pressure)

Nutation in Obliquity

Period (day)	standard	$\Delta\mu$ (5%)	ΔK (2%)	$\Delta\mu, \Delta K$
			parameter	
686.72	-0.0493	-0.0493	-0.0493	-0.0493
343.41	0.5158	0.5158	0.5158	0.5158
228.96	0.1130	0.1130	0.1130	0.1130
171.72	0.0193	0.0193	0.0193	0.0193
137.38	0.0030	0.0030	0.0030	0.0030
686.93	-0.0004	-0.0004	-0.0004	-0.0004
828.5	-0.0040	-0.0040	-0.0040	-0.0040
19850	-0.0028	-0.0028	-0.0028	-0.0028

Nutation in Longitude

Period (day)	standard	$\Delta\mu$(5%)	ΔK (2%)	$\Delta\mu, \Delta K$(2%)
			parameter	
686.80	-0.1407	-0.1407	-0.1407	-0.1407
343.43	1.0962	1.0962	1.0962	1.0962
228.96	0.2401	0.2401	0.2401	0.2401
171.72	0.0409	0.0409	0.0409	0.0409
137.38	0.0634	0.0634	0.0634	0.0634
114.48	0.0009	0.0009	0.0009	0.0009
686.93	-0.6357	-0.6357	-0.6357	-0.6357
343.46	-0.0445	-0.0445	-0.0445	-0.0445
228.98	-0.0041	-0.0041	-0.0041	-0.0041
828.5	-0.23	-0.23	-0.23	-0.23
19850	-0.060	-0.060	-0.060	-0.060

All models were calculated with a core diameter of 1700 km.

The only parameter which causes a significant change in the amplitudes of the nutation components is the change in Mars' principal moment of inertia. The source of the change in the amplitudes, however, is the indirect proportionality of the amplitude of a nutation component to the inertia ratio, q, in the rigid Mars model. The change in the amplitudes caused by the change in the inertia ratio for the solid core models are actually greater than they are for the liquid core models. The smaller change in amplitudes of the nutation components for the liquid core models shows that, for the liquid core models, along with the change in the inertia ratio, there is also a change in the planet's elasticity. This change in elasticity partially offsets the change in the amplitude caused by the change in the inertia ratio for a rigid planet.

Overall, the solid core models have little ability to determine the size of Mars' core, but they are better at determining the inertia ratio than the liquid core models. However, the inertia ratio is easily determined from gravitational field measurements, as shown by Reasenberg (1977), although the present value for the inertia ratio does depend on the particular planetary model being used (Bills 1989).

4. METHODS OF DETERMINING THE MOTION OF MARS' POLE

There have been few attempts (e.g., Borderies *et al.* 1980) to measure the precession and nutation of solar system bodies aside from the Earth. There have been no attempts to measure the polar motion of other planets. The reason so few attempts to measure precession and nutation have been made is because the measurement of nutation and the Chandler wobble period require data to be taken over a long period of time and the orientation of the planet needs to be known to a high precision. To achieve milliarcsecond precision for all of Mars' nutation components ⩾0″001 in amplitude, the horizontal displacement of the surface at the equator needs to be known to an accuracy of 1.6 cm over a period of 54.34 years! To measure the 11 nutation components of Mars that are larger than 10 milliarcsec to an accuracy of

0."01 requires the orientation of the planet to be known to 16 cm for a period of 1.881 years.

4.1 Methods of Collecting Data

Methods of collecting data on the orientation of Mars can be divided into three categories. (1) Indirect, Earth-based determinations such as radio and radar ranging, (2) indirect space-based determinations using observations of an artificial satellite near Mars, and (3) direct, Mars-based determinations such as the use of a Mars-based photographic zenith tube.

4.1.1 Earth-based methods

The Earth-based methods for observing the orientation of Mars are (1) passive observation of the planet through telescopes and (2) active methods such as ranging information with a radio transponder as done in the Viking program and radar ranging.

Telescopic observations of Mars have been made ever since the invention of the telescope. They have provided orientation information such as the rate of revolution of Mars to an accuracy of 0.0026 s of time and the position of the rotational pole to 0."01 (de Vaucouleurs 1964). To achieve this accuracy, however, has required nearly ninety years of observations. To achieve milliarcsecond precision from telescopic observations requires an improvement of 4.6 orders of magnitude over previous observations. The determination of the motion of Mars' pole also requires a long series of regular observations, so neither short period variations nor the highly accurate determinations of the orientation of Mars are possible from telescopic observation.

The most accurate ranging data that exists for Mars are the radio transponder ranges made using the Viking landers. These data represent the most accurate distance measurement data available, having one way accuracies of 1–5 m over distances on the order of 10^{11} m (Reasenberg & King 1979). This accuracy is equivalent to a displacement of 0."06–0."30 at the equator of Mars. However, the raw data are somewhat misleading for their use in determining changes in orientation. First, the uncertainty in the range is directly translatable to the uncertainty in the planet's orientation only when the lander is on the limb of the planet and then only for changes in longitude. When the lander is supposed to be directly on the Earth–Mars line, it would take a rotation of Mars of approximately 160″ at mean opposition to produce a 1 m change in the range. Second, there are large (~ 60 day) gaps in the Viking ranging data during the times when Mars was too close to the Sun for accurate ranging. Other problems involved in ranging include (1) modeling the electronics time delay in the transponder, (2) density changes in the solar wind which affect the velocity of the electromagnetic waves, especially when the Sun is near the Earth–Mars line, and (3) the ranging information determines the position of Mars relative to the observer so the orientation of the Earth as well as the orientation of Mars is convolved in the data. Therefore, an accurate determination of the orientation of Mars from ranging data requires sophisticated deconvolution.

Borderies et al. (1980) shows both the difficulties inherent in using Viking data and the potential of radar ranging to determine the amplitudes of nutation and the Chandler wobble for Mars. Their data, which have been corrected for rigid planet nutation, show definite periodic residuals. However, the scatter in the data is large and the time period covered by the data is short; thus, it is not possible to determine if the residuals are from a single nutation or normal model (e.g., the signature of a fairly large Chandler wobble) or from multiple nutation components or simply result from some systematic error in the data.

4.1.2 Space-based methods

The second method of indirect determination of the precession and nutation of Mars is to observe the motion of a satellite circling the planet. Since the orbit of a satellite around a planet is determined by the planet's gravitational field, a change in the orientation of the planet will cause a change in the satellite's orbit. Thus, an observer not on the planet, able to determine the orientation of the satellite orbit with sufficient accuracy, over a long enough period of time, can convert the orbit information into a measure of the motion of the planet's pole. An observer on the planet that a satellite is orbiting also has to include additional geometric effect of the motion of the platform. For example, the geometric effect of precession just cancels out the dynamic effect on the satellite, so it is impossible to observe from the Earth the effect of the Earth's precession on Earth-orbiting satellites.

To determine the polar motion of the planet the long-period changes in the orbit's orientation that would appear on top of the short-period changes caused by the movement of the satellite through the gravitational field of the planet need to be observed. Variations caused by the gravitational field can be minimized by putting a satellite in synchronous equatorial orbit. The chief difficulties in using observations of satellite orbits for the motion of the Earth's pole are (1) secular changes in the satellite's orbit from atmospheric drag and (2) the effects of long-period ocean tides that look the same as nutation. Smith et al. (1990) have already modeled the effect of atmospheric drag for the low-orbiting Mars Observer mission. There are no oceans to cause additional long-term tidal effects. Thus, the two largest sources of error in determining the Earth's polar motion from satellite observations have been addressed for the satellite determination of Mars' polar motion. Mars will also cause a larger change in the orbit of a satellite for a given change in orientation than the Earth because of Mars' greater dynamical oblateness.

The ability to collect the high precision data needed to determine the polar motion of Mars with present technology is shown to be possible, at least over short timescales, by Christiansen & Balmino (1979), who used orbital ranging data to Mariner 9 and the Viking orbiters to determine a twelfth degree and order model for the gravitational field of Mars, while Mars Observer is expected to determine Mars' gravitational field to the fiftieth degree and order over the two year lifetime of its mission (Smith et al. 1990). Thus, the use of artificial satellites to determine the polar motion of Mars is a strong possibility. Mars Observer is one potential source of orientation information.

4.1.3 Mars-based methods

A Mars-based determination of its orientation can be done using the same instruments that are used for direct measurement of the Earth's orientation (1) polar telescopes, (2) radio interferometry, and (3) photographic zenith tubes.

A polar telescope, as the name implies, is designed to point toward the pole of rotation at all times. This telescope observes the diurnal trails of close circumpolar stars (Roches-

ter *et al.* 1974). Hence, a polar telescope can be used to directly observe both the precession and nutation of the Martian pole. However, such an instrument would have to be located at a high latitude to minimize refraction effects of the Martian atmosphere. Atmospheric refraction and the inhospitable climate at very high latitudes on the Earth have led to very limited use of polar telescopes on Earth. Except for occasional dust storms, Mars' atmosphere is much clearer than the Earth's and it has a lower index of refraction, since it is only about 1/100 as dense. The main drawback of polar telescopes is that they are insensitive to changes in the latitude of the observatory. This insensitivity to latitude changes makes the nutation of the planet easier to observe, but the Chandler wobble can not be observed. Overall, the polar telescope is a very good instrument for observing the precession, nutation, and FCN, but not the Chandler wobble.

Very long base line interferometry and connected element interferometry are the most accurate methods of determining the Earth's orientation in space. Using these techniques, it is possible to obtain results that are accurate at the submilliarcsecond level (e.g., Himwich & Harder 1988; Herring *et al.* 1988). However, radio interferometry requires multiple sites, massive amounts of equipment (including radio antennae with apertures that are tens of meters in diameter), and well coordinated observing schedules. The equipment and timing requirements make radio interferometry difficult to accomplish on the Earth and would make such observations impossible on another planet such as Mars.

Finally, there is the photographic zenith tube (PZT). This is a combination refractor-reflector telescope designed to observe stars as they pass directly through the zenith at the observatory's location. In a PZT the light passes through a refracting lens that is parallel to the ground, bounces off a pool of mercury, and is then focused on a detector located directly behind the refracting lens. Nutation is determined from the north–south change in the chord that the observed stars make between observations (latitude) and the change in the time of passage of the stars (longitude). Precession is measured by the secular drift of the stars with time. Polar motion appears as changes in the position of the center of the arc of motion of the observed stars. McCarthy (1980) shows that, with proper reduction, the accuracy of individual PZT plates can be as high as $0\rlap{.}''01$. This accuracy represents an upper bound on the accuracy obtainable from a Mars-based PZT, since no Earth-based PZT has made use of recent improvements in technology such as the CCD, and the size of the stellar image by the Martian atmosphere would be much smaller than the image produced by the Earth's atmosphere. The technological improvements have not been made to PZTs because radio interferometry methods are superior to the PZT for making Earth orientation measurements, rather than any unsuitability of the technology. The seeing disk for a PZT on Mars would be smaller because the Martian atmosphere is much thinner than the Earth's and would produce less turbulence. Since the PZT observes solely at the zenith, the problems of atmospheric refraction are minimized. Finally, the operation of a PZT is routine and easily automated.

Overall, the Mars-based methods of determining the precession and nutation of the planet are the most desirable. First, the Mars-based methods do not require the separation of other sources of motion included in the indirect methods of measuring polar motion. Second, the direct methods rely on simple, well developed, highly accurate devices. Some of

these devices, such as the PZT, would produce results superior to the results produced on the Earth because of local conditions such as Mars' thinner atmosphere. There is also room for technological improvement in these devices such as the use of CCDs instead of photographic plates in PZTs. Third, although the instruments would need to be placed on the surface of Mars, both the PZT and the polar telescope are simple enough to be relatively inexpensive to deploy. Besides, any significant improvement in the knowledge of Mars' orientation in space will require the placement of some sort of device either in Mars' orbit or on its surface.

4.2 Precession and Nutation of Other Planets

As demonstrated in Sec. 3 observing the motion of Mars' pole is a useful probe of its structure. There is no basic physical reason why such a method cannot be used as a probe of the structure of other planets as well. It is worthwhile to take a look at the other planets in the solar system and try to determine those planets for which this technique might be useful. The numerical quantities used in this section unless otherwise attributed are taken from the Astronomical Almanac for the Year 1992 (1991).

Mercury is believed to have a liquid core that is large in comparison to its mantle. It should therefore show very large core effects in the motion of its pole. In addition, Mercury's short distance from the Sun and its eccentric orbit indicate that it should have large precession and nutation. However, Mercury rotates slowly, completing one sidereal rotation in 58.646 days. Since this rate of rotation is in a 3-to-2 resonance with its orbital period, the amplitudes of some of its nutation components may actually be enhanced by the resonance between its orbital period and its rotation rate. Its slow rate of rotation also means, however, that the planet is nearly spherical, so there is very little difference between the polar and equatorial moments of inertia to drive the motion of the planet's pole. The J_2 coefficient of the potential for Mercury is unknown, but the measured geometric flattening is 0. Also, the inclination of Mercury's equator to its orbit is only about $0\rlap{.}°01$. Finally, Mercury does not have any satellites to aid in driving precession and nutation, so it is doubtful that the motion of Mercury's pole is significant.

Venus, like Mercury, has the advantage of being close to the Sun, so that the Sun's mass can be a significant driver of precession and nutation. However, also like Mercury, Venus rotates very slowly on its axis with a sidereal period of 243.0 days. Venus' J_2 gravitational coefficient is only 2.5% that of the Earth's. However, because its rotation is retrograde rather than direct, its solar diurnal period is 116.7 days. Venus also has an absolute inclination of its equator to its orbit of $2\rlap{.}°66$. The basic formula for the precession of a rigid body [Eq. (28) Hilton 1991], with the parameters for Venus, gives a precessional motion of $270''$ per year. This number is deceptively large because this is the motion of the pole around the small circle it traces on the sky. In terms of the actual motion in seconds of arc on the sky, the precession is only $270'' \sin 2\rlap{.}''66 = 13''$ in comparison to $50\rlap{.}''291 \times \sin 23\rlap{.}''439 = 20\rlap{.}''005$ for the Earth and $7\rlap{.}''295 \sin 25\rlap{.}''20 = 3\rlap{.}''106$ for Mars. Knowledge of Venus' precession only determines the values of its principal moments of inertia, which are more easily determined by other methods. However, the size of Venus' nutation must be small because its orbit is the most nearly circular of the planets, so solar driven nutation will be small and there is no satellite to help drive

precession and nutation. Therefore, despite its closeness to the Sun, Venus must have small nutation terms and a precession that is smaller in terms of the motion on the sky than the Earth's. Detection of the precession and nutation of Venus would also be difficult because of its cloudy atmosphere. It would be impossible to observe changes in Venus' orientation from its surface except at radio wavelengths. The only reasonable method of determining the precession and nutation is the observation of a satellite in orbit about Venus. This method would be difficult to accomplish because Venus' small J_2 means that a change in Venus' orientation would cause only a small change in the satellite's orbit. Thus, the prospects of observing the precession and nutation of Venus are also poor.

Jupiter, like all of the gas giant planets, cannot be described as having a definite surface. Therefore, any observation of its precession and nutation would have to be done by observing the effect of the motion of its pole on a spacecraft, such as Galileo, in orbit about it. The inner structure of the planet is believed to be the inverse of the terrestrial planets, consisting of a solid core surrounded by a liquid mantle. Smith (1977) has shown that the methods used for analyzing the polar motion of a planet with a liquid core can easily be extended to the case of a planet with a liquid mantle, and Smith (1976) shows how extensions of the normal mode method is used to analyze the effects of a solid inner core on the motion of the Earth. Thus, the techniques for studying the effects of a planet with a solid core and a liquid mantle on the motion of its poles already exist. One of the problems in analyzing the motion of the Earth (Wahr 1982) is the division of the effects into tidal and nutational components. This problem disappears for Jupiter, since the entire mantle of the planet would be seen to shift in a single tide-nutation term. Jupiter has two further properties that lend it to polar motion analysis. (1) It has a very large value for J_2 (0.01475) and (2) it has a small inertia ratio (0.25; Fish 1967). Despite these advantages, it is expected that the motion of Jupiter's pole are rather small. The precession and nutation driven by the Sun will be small because Jupiter's equator is tilted only 3°.13 degrees to its orbit and its distance from the Sun is 5.2 AU. Using the values for J_2 and the inertia ratio for Jupiter, a zeroth order estimate for the Jovian precession driven by the Sun in terms of its motion on the sky is only 0″.92 per year. Also, all of the Galilean satellites have orbits with mean inclinations of less than a degree to Jupiter's equator. However, as shown in the case of Mars, it is possible for such low inclination satellites to drive significant long-period nutation components. A combined Chandler wobble FCN (Smith 1976) should be easily detectable; that is, the normal modes of the planet, rather than the forced nutation, would be the source of the greatest information. Since the structural situation of Jupiter is the reverse of the terrestrial planets, other normal modes that are restricted to the Earth's core should be observable on Jupiter. This means an additional method of determining the structure of Jupiter is to study the other normal mode oscillations using Jovian seismology (Schmider et al. 1991).

The increasing distance from the Sun and the major satellites' preference to orbit Saturn and Uranus in planes near the equator of the planets make it difficult to drive precessions and nutation that would be detectable for either of these two planets. However, observations of the normal mode oscillations of these planets, like the observations suggested for Jupiter, is a possibility.

The only exception to the prospect of small nutation amplitudes among the outer gaseous giant planets is Neptune. Neptune's largest satellite, Triton, is approximately the size of the Moon and orbits Neptune at 92% of the Moon's distance from the Earth. Also, like the Moon, Triton's orbit is inclined to Neptune's equator (159°.00). This combined with Neptune's large J_2 (0.004) and small inertia ratio (0.29; Fish 1967) gives a zeroth order estimate for the precession caused by Triton of 40″ per year. Although Triton's orbit is nearly circular, there should also be at least one large nutation associated with the motion of the node of Triton's orbit. However, the motion of the node itself should be slow because of the low eccentricity of the orbit. The main problem in observing Neptune is its remoteness; otherwise, it would be the best giant planet candidate for observation of precession and nutation.

Pluto is so remote from the Sun that its solar-driven precession and nutation is extremely small. In addition Pluto's only known satellite, Charon, although massive and close to Pluto, is in an orbit that is totally evolved rotationally, making it useless as a driver of precession and nutation. Finally, Pluto is so extremely remote that observations of precession and nutation are impossible with present technology.

5. CONCLUSIONS

There are seven conclusions to be drawn from this study of the effect of planetary structure of the motion of Mars' pole.

(1) The inertia ratio, q, of Mars, that is the polar principal moment of inertia divided by the mass times the equatorial radius squared, is most likely to be near 0.3654 (Reasenberg 1977). The more centrally condensed value, $q = 0.345$ (Bills 1989) is not as likely because the hydrostatic polar and equatorial radii for the less centrally condensed, larger q, models more closely resemble the measured polar and equatorial radii of the planet.

(2) The effect of the possible off-center position of the core (Reasenberg 1977) and other core-mantle boundary relief effects are too small to affect the nutation at the 0″.001 level.

(3) The effect of the structure of Mars on precession and nutation is significant only for the case of a liquid core. The Mars models produce a planet that is more rigid than the Earth. Because of the increased planetary rigidity, the Chandler wobble period of Mars is not as sensitive to either the existence of a liquid core or the change from rigid mantle to elastic mantle models as these same changes are in the models for the Earth's Chandler wobble. If the period of the Martian Chandler wobble is known with the same accuracy as the period of the Earth's Chandler wobble, then the low sensitivity of Mars' Chandler wobble period means that the uncertainty in the core radius is 180 km. The period of the Chandler wobble is also highly nonlinear with core radius and produces a unique value for the core radius for only a restricted range in its period.

(4) The increased rigidity of the mantle also leads to a lower value for the quality factor for Mars' normal modes of oscillation. Therefore, a nutation frequency can be farther from one of Mars' normal modes and still show a greater change in the amplitude from the rigid body solution than a similar nutation of the Earth would. As a result, the amplitudes of the nutation components of Mars show a significant

amplitude change with change in the core size. The sensitivity is high enough that, if the measured amplitudes of the nutation components are accurate to 0.″001, the uncertainty in the core size would be 32 km for the largest nutation in longitude. The nutation in longitude driven by the motion of Phobos' node may also be usable as a probe of the interior of the planet. However, the two main sources of uncertainty (the rate of motion of the node and Phobos' mass) need to be known to higher accuracy.

(5) The free-core nutation period is found to be a sensitive, nearly linear function of the mean core radius. A determination of the period of the FCN to an accuracy of 2 days produces an uncertainty in the core radius of only 6 km. In all cases the amplitude of the nutation components and the periods of the Chandler wobble and free-core nutation were several times more sensitive to the size of the core than they were to the uncertainty in any other parameter, such as the rigidity and bulk modulus of the Martian mantle and the inertia ratio of Mars.

(6) Present technology is sufficient to obtain the data necessary to determine whether the planet has a solid or a liquid core. If the core is liquid, its mean radius can be determined to an uncertainty of at most 25 km and possibly as small as 6 km.

(7) The ability of polar motion observations to determine the interior structure of Mars gives rise to the question of whether this method can be used for other planets in the solar system. A preliminary appraisal of the other planets shows that Jupiter and Neptune are the only other candidates for which precession and nutation might be significant. The lack of significant precession and nutation in the other planets results from one or more of the following: (1) having a nearly spherical mass distribution; (2) too remote for the Sun to drive significant precession and nutation; and (3) the obliquity with respect to those other gravitational sources that could drive precession and nutation is very low. A more thorough study would have to be made on both Jupiter and Neptune to determine their suitability for nutation studies because they are both marginal cases. Jupiter, Saturn, Uranus, and Neptune, however, may all have significant polar motion. It has also been suggested for the giant planets, that the observation of the other normal modes of oscillation that are confined to the cores of the terrestrial planets can be studied as a probe of their interiors.

Overall, the observation of the polar motion of Mars would lead to a much better understanding of the structure of the planet and give a better notion of the similarities and differences between the terrestrial planets in the solar system. The study of the motion of the pole by observing the changes in the orbits of artificial satellites around the giant planets such as Jupiter is one method to study the interior structure of these planets.

REFERENCES

Anderson, D. L., *et al.* 1977, J. Geophys. Res. 82, 4524

The Astronomical Almanac for the Year 1992, 1991, The Nautical Almanac Office of the United States Naval Observatory (U.S. Government Printing Office, Washington, DC)

Bills, B. G. 1989, Geophys. Res. Lett. 16, 385

Binder, A. B., & Davis, D. R. 1973, Phys. Earth Planet. Inter. 7, 477

Borderies, N., Balmino, G., Castel, L., & Moynot, B. 1980, Moon Planets, 22, 191

Bullard, E. C. 1948, MNRAS, Geophys. Suppl., 5, 186

Chandler, S. C. 1891, AJ, 11, 59

Christensen, E. J., & Balmino, 1979, J. Geophys. Res., 84, 7943

Clairaut, A. C. 1743, Théorie de la Figure de la Terre, Tirée des Principes de l'Hydrastatique (Durand, Paris)

Dahlen, F. A. 1972, Geophys. J. Roy. Astron. Soc., 28, 357

Dahlen, F. A. 1976, Geophys. J. Roy. Astron. Soc., 46, 363

Dahlen, F. A., & Smith, M. L. 1975 Philos. Trans. Roy. Soc. London, Ser. A, 279, 583

Davies, M. E., *et al.* 1985, Report of the IAU/IAG/COSPAR Working Group on Cartographic Coordinates and Rotational Elements of the Planets and Satellites: 1985, reprinted in Celest. Mech., 39, 103 (1986)

de Vaucouleurs, G. 1964, Icarus, 3, 236

Fish, F. F. 1967, Icarus, 7, 251

Herring, T. A., Gwinn, C. R., Buffett, B. A., & Shapiro, I. I. 1988, in The Earth's Rotation and References Frames for Geodesy and Geodynamics, IAU Symposium No. 128, edited by A. K. Babcock and G. A. Wilkins (Reidel, Boston), p. 293

Hestenes, D. 1986, New Foundations for Classical Mechanics (Kluwer, Boston)

Hilton, J. L. 1990, Ph. D. dissertation, University of Texas, Austin

Hilton, J. L. 1991, AJ, 102, 1510

Himwich, W. E., & Harder, E. J. 1988, in The Earth's Rotation and Reference Frames for Geodesy and Geodynamics, IAU Symposium No. 128, edited by A. K. Babcock and G. A. Wilkins (Kluwer, Boston), p. 301

Hough, S. S. 1895, Philos. Trans. Roy. Soc. London, Ser. A, 186, 469

Hough, S. S. 1896, Philos. Trans. Roy. Soc. London, Ser. A, 187, 319

Johnston, D. H., & Toksoz, M. N. 1977, Icarus, 32, 73

Kaula, W. M., Sleep, N. H., & Phillips, R. J. 1989, Geophys. Res. Lett., 16, 1333

Kinoshita, H., & Souchay, J. 1900, Celest. Mech., 48, 187

Larmor, J. 1909, Proc. Roy. Soc. London, Ser. A, 82, 89

Longman, I. M. 1962, J. Geophys. Res., 67, 845

Longman, I. M. 1963, J. Geophys. Res., 68, 485

Lorell, J., *et al.*, 1972, Sci., 175, 317

Love, A. E. H. 1909, Proc. Roy. Soc. London, Ser. A, 82, 73

McCarthy, D. D. 1980, Publ. Inter. Latitude Obs. Mizusawa, 14, No. 1, 1

Melchior, P. 1986, The Physics of the Earth's Core: An Introduction (Pergamon, Oxford)

Okal, E. A., & Anderson, D. L. 1978, Icarus, 33, 514

Ooe, M. 1978, Geophys. J. Roy. Astron. Soc., 53, 445

Phinney, R. A., & Burridge, R. 1973, Geophys. J. Roy. Astron. Soc., 34, 451

Poinsot, L. 1852, Théorie Nouvelle de la Rotation des Corps (Bachelier, Paris)

Reasenberg, R. D. 1977, J. Geophys. Res., 82, 369

Reasenberg, R. D., & King, R. W. 1979, J. Geophys. Res., 84, 6231

Rochester, M. G. 1970, in Earthquake Displacement Fields and the Rotation of the Earth, edited by L. Mansinha, D. E. Smylie, and A. E. Beck (Reidel, Dordrecht), p. 136

Rochester, M. G., Jensen, O. G., & Smylie, D. E. 1974, Geophys. J. Roy. Astron. Soc., 38, 349

Schmider, F.-X., Mosser, B., & Fossat, E. 1991, A&A, 248, 281

Seidelmann, P. K., *et al.* 1981, 1980 IAU Theory of Nutation: The Final Report of the IAU Working Group on Nutation, reprinted in Celest. Mech., 27, 79 (1982)

Smith, D. E., Lerch, F. J., Chan, J. C., Chinn, D. S., Iz, H. B., Mallama, A., & Patel, G. B. 1990, J. Geophys. Res. 95, 14155

Smith, J. C., & Born, G. H. 1976, Icarus, 27, 51

Smith, M. L. 1974, Geophys. J. Roy. Astron. Soc., 37, 491
Smith, M. L. 1976, J. Geophys. Res., 81, 3055
Smith, M. L. 1977, Geophys. J. Roy. Astron. Soc., 50, 103
Smith, M. L., & Dahlen, F. A. 1981, Geophys. J. Roy. Astron. Soc., 64, 223
Stacey, F. D. 1977, Physics of the Earth, 2nd ed. (Wiley, New York), p. 172
Struve, H. 1898, Mem. Acad. Imp. Sci. St. Petersbourg, Ser. VIII, 3, 66

Wahr, J. M. 1979, Ph. D. dissertation, University of Colorado
Wahr, J. M. 1981a, Geophys. J. Roy. Astron. Soc., 64, 651
Wahr, J. M. 1981b, Geophys. J. Roy. Astron. Soc., 64, 705
Wahr, J. M. 1982, Geophys. J. Roy. Astron. Soc., 70, 349
Wahr, J., & de Vries, D. 1989, Geophys. J. Int., 99, 511
Zhu, S., Y., Groten, E., & Reigber, Ch. 1990, AJ, 99, 1024